AD 741457

UNITED STATES AIR FORCE

AIR UNIVERSITY

AIR FORCE INSTITUTE OF TECHNOLOGY

Wright-Patterson Air Force Base, Ohio

D D C

RECEIVED

MAY 18 1972

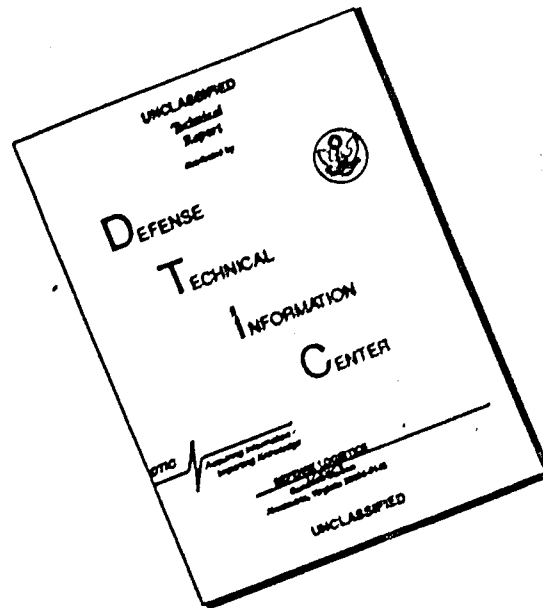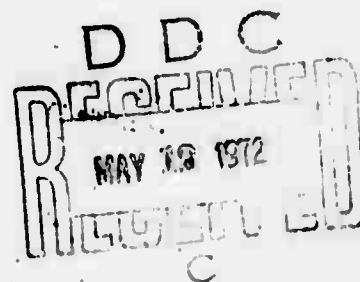C

DISCLAIMER NOTICE

THIS DOCUMENT IS BEST QUALITY AVAILABLE. THE COPY FURNISHED TO DTIC CONTAINED A SIGNIFICANT NUMBER OF PAGES WHICH DO NOT REPRODUCE LEGIBLY.

A COMPARISON OF THE EXTENDED KALMAN
FILTER AND WEIGHTED LEAST SQUARES
IN EARLY-ORBIT DETERMINATION

THESIS

Jackson R. Ferguson, Jr.
GA/EE/72S-1   Captain   USAF

DOCUMENT CONTROL DATA - R & D

(Security classification of title, body of abstract and indexing annotation must be entered when the overall report is classified)

1. ORIGINATING ACTIVITY *(Corporate author)*	2a. REPORT SECURITY CLASSIFICATION
Air Force Institute of Technology Wright-Patterson Air Force Base, Ohio 45433	2b. GROUP

3. REPORT TITLE

A Comparison of the Extended Kalman Filter and Weighted Least Squares in Early-Orbit Determination

4. DESCRIPTIVE NOTES *(Type of report and inclusive dates)*

AFIT Thesis

5. AUTHOR(S) *(First name, middle initial, last name)*

Jackson R. Ferguson, Jr.
Captain   USAF

6. REPORT DATE	7a. TOTAL NO. OF PAGES	7b. NO. OF REFS
December 1971	74	8

8a. CONTRACT OR GRANT NO.	9a. ORIGINATOR'S REPORT NUMBER(S)
8b. PROJECT NO.	
N/A	GA/MC-72S-1
c.	9b. OTHER REPORT NO(S) *(Any other numbers that may be assigned this report)*
d.	

10. DISTRIBUTION STATEMENT

This document has been approved for public release and sale; its distribution is unlimited.

11. SUPPLEMENTARY NOTES	12. SPONSORING MILITARY ACTIVITY
Approved for release IAW AFR 190-17 STEPHEN B. INGRAM, Captain, USAF Director of Information, AFIT	

13. ABSTRACT

The problem of estimating the orbit parameters from early-orbit observations of an earth satellite is used to compare the accuracy and application of the Extended Kalman filter and the classical filtering method of Weighted Least Squares. To obtain an absolute comparison, a true two-body, drag-free Keplerian orbit is simulated, observations are computed and contaminated with noise, and the orbit parameters estimated by each filter are compared. The accuracy of the two filters was compared using the same set of observations to determine the effect of observation truncation and initial conditions on the results. Based on this study it was concluded that the Weighted Least Squares filter and the Extended Kalman filter yield about the same accuracy in the early-orbit determination problem.

DD FORM **1473** Nov 65

KEY WORDS	LINK A		LINK B		LINK C	
	ROLE	WT	ROLE	WT	ROLE	WT
Early-orbit						
Orbit determination						
Two-body						
Extended Kalman filter						
Weighted Least Squares						
Differential correction						
Filtering						

A COMPARISON OF THE EXTENDED KALMAN

FILTER AND WEIGHTED LEAST SQUARES

IN EARLY-ORBIT DETERMINATION

THESIS

.

Presented to the Faculty of the School of Engineering

of the Air Force Institute of Technology

Air University

in Partial Fulfillment of the

Requirements for the Degree of

Master of Science

by

Jackson R. Ferguson, Jr., B.S.E.S.

Captain   USAF

Graduate Astronautics

December 1971

Preface

This thesis is a continuation of the work done by Captains Charles E. Rogers and Christo Christodoulou, AFIT-ENE, GE-71S in the application of the Extended Kalman filter to orbit determination. The Extended Kalman filter is compared to the Weighted Least Squares

I would like to express my appreciation and thanks to Lt. Col. Russell A. Hannen, AFIT-ENE, my sponsor, for his advice and instruction in estimation theory; Major James E. Funk, AFIT-ENE, for his advice and instruction in guidance and control; Captain Richard C. Walsh, Det 1, AFSCF, for his material and advice concerning Weighted Least Squares; and Captains Rogers and Christodoulou for their help in understanding the Extended Kalman filter computer program. Finally, I would like to thank my wife, Christina for her help and understanding in the preparation of this report.

<div style="text-align: right">Jackson R. Ferguson, Jr.</div>

Contents

List of Figures

List of Tables

List of Symbols

a	Azimuth
E[ ]	Expected value
e	Elevation
F	State sensitivity matrix
$\underline{f}(),\underline{h}()$	Vector valued function
K	Kalman gain matrix
M	Measurement matrix
n	Number of observations
P	State error covariance matrix
R	Measurement error covariance matrix
r	Radius of the satellite
t_0	Initial time
t	Time from t_0
t_f	Final time
v	Inertial velocity of the satellite
x,y,z	Geocentric satellite coordinates
$\underline{x}$	System state vector
$\underline{y}$	$4n \times 1$ measurement vector
$\underline{z}$	4×1 measurement vector
θ	Station longitude
μ	Universal gravitation constant times Earth mass
ρ	Slant range
$\dot{\rho}$	Slant range rate
Φ	State transition matrix
φ	Station latitude
ω	Earth rotation rate (radians/second)

Subscripts

I	Inertial geocentric system
R	Rotating geocentric system
S	Station coordinates in rotating geocentric system
T	Rotating topocentric system

Superscripts

^	Estimate
T	Transpose
-1	Inverse

Abstract

The problem of estimating the orbit parameters from early-orbit observations of an earth satellite is used to compare the accuracy and application of the Extended Kalman filter and the classical filtering method of Weighted Least Squares. To obtain an absolute comparison, a true two-body, drag-free Keplerian orbit is simulated, observations are computed and contaminated with noise, and the orbit parameters estimated by each filter are compared. The accuracy of the two filters was compared using the same set of observations to determine the effect of observation truncation and initial conditions on the results. Based on this study it was concluded that the Weighted Least Squares filter and the Extended Kalman filter yield about the same accuracy in the early-orbit determination problem.

A COMPARISON OF THE EXTENDED KALMAN

FILTER AND WEIGHTED LEAST SQUARES

IN EARLY-ORBIT DETERMINATION

I. Introduction

The determination of the orbit parameters of man-made satellites
usually involves the calculation of the satellite's position and
velocity at some epoch time using a number of observations from the
earth's surface. These observations are inherently noisy, so the
determination of the orbit parameters is a statistical problem, thus
a "best" estimate of the orbit parameters is obtained using some form
of a statistical filter.

One of the traditional methods of solving this filter problem is
via differential correction of initial conditions using the classical
method of Weighted Least Squares (WLS). This method produces a very
good estimate of the orbit parameters when a large number of observa-
tions are available, i.e., when the system is highly overdetermined.
Problems arise when the number of observations is small, thus one of
the goals of this study is to investigate the application of the WLS
filter to early-orbit determination. Early-orbit determination is
extremely important as the orbit parameters must be quickly and
accurately obtained in order to generate pointing data for subsequent
tracking stations and to determine contingency actions if the orbit
is unsatisfactory.

A recent development in estimation theory is the application of the Extended Kalman filter to the early-orbit determination problem (Ref 3). The Extended Kalman filter yields estimates of the orbit states and parameters via sequential processing of a set of noisy observations.

The purpose of this study is to compare the accuracy and ease of application of the Weighted Least Squares filter and the Extended Kalman filter when applied to the early-orbit determination problem. The application of the Weighted Least Squares filter to orbit determination is described in Reference 7. Previous studies considered the application of the Extended Kalman filter to single orbit (Ref 3) and multiple orbit (Ref 8) radar tracking observations of actual earth satellites. The radar tracking data for these Kalman filter studies were obtained from the Space Detection and Tracking System (SPADATS). Although the results of these two studies using the Kalman filter compared favorably with the orbit parameters determined by SPADATS using a Weighted Least Squares filter, the results did not give an absolute comparison of the Kalman filter with the WLS filter as the true orbit parameters were unknown. This uncertainty in orbit parameters is due to the fact that an actual earth satellite is subjected to perturbations such as the effect of a non-spherical earth, atmospheric drag and magnetic field drag. These small perturbations and small long term changes in orbit cause changes which were not accurately modeled by the Extended Kalman filter nor by the WLS filter.

Therefore, in this study, a true two-body Keplerian orbit is simulated, observations are computed and contaminated with noise, and

the orbit parameters estimated by each filter are compared. In this way, both an absolute and relative comparison can be made of the actual orbit parameters and estimated orbit parameters produced by the two filters. Here the WLS filter as described in Reference 7 and the Extended Kalman filter as described in Reference 4 are used.

The following assumptions are made concerning the two-body Keplerian orbit:

1. The satellite is a point mass under the gravitational attraction of a spherical rotating earth with negligible atmospheric drag and magnetic field drag.

2. The satellite is non-thrusting.

The following assumptions are made concerning the observations of the orbit:

1. Uncertainties in latitude, longitude and height of the tracking sensors are assumed negligible.

2. The noise in the observation is assumed to be an additive, zero-mean, white, Gaussian sequence.

This report is divided into seven chapters plus three appendices. Chapter II includes an explanation of the coordinate systems used, the required coordinate transformations, a description of the equations of motion, the method of determining the initial conditions, and the method used to generate the noisy tracking data. In Chapter III, the Extended Kalman filter equations and the linearization procedure used by this filter are described. Chapter IV describes the Weighted Least Squares method and the linearization procedure used in this filter. Chapter V gives a comparison of the application of the two filters and details their relative advantages and disadvantages. A description of

3

the data and an analysis of the results obtained are in Chapter VI
followed by the conclusions and recommendations in Chapter VII. The
equations for determining the initial position and velocity are
described in Appendix A; Appendix B contains a description of the
system sensitivity matrix and the measurement matrix description is
presented in Appendix C.

II. The Model

Coordinate Systems

Three coordinate systems are involved in the orbit determination problem: the inertial geocentric system and the rotating geocentric system have as their origin the center of the earth, while the rotating topocentric system has its origin on the surface of the earth at the location of a tracking station. The three systems are shown in Figure 1 and are described in detail below.

Inertial Coordinate System. The center of the inertial coordinate system is the center of the earth. The principal axis, X_I, is directed toward the first point of Aries, γ. The Y_I axis is directed perpendicular to X_I in the equatorial plane, while Z_I is toward the earth's north pole. The equations of motion employed in the WLS method are written in this system because orbital motion is most readily expressed in inertial space.

Rotating Geocentric System. As with the inertial system, the center of the earth is the origin of the rotating geocentric system. The principal axis, X_R, is toward the earth's prime meridian, Greenwich, and Y_R and Z_R are defined similarly to Y_I and Z_I. The difference between the two systems is that the rotating system rotates about the Z_R axis at earth rotation, ω. The equations of motion used in the Kalman filter are expressed in this system in order to simplify the transformation to the topocentric system.

Rotating Topocentric System. The origin of the rotating topocentric system is the antenna of the tracking station. The principal axis, X_T, is toward local North in the plane tangent to the earth at

5
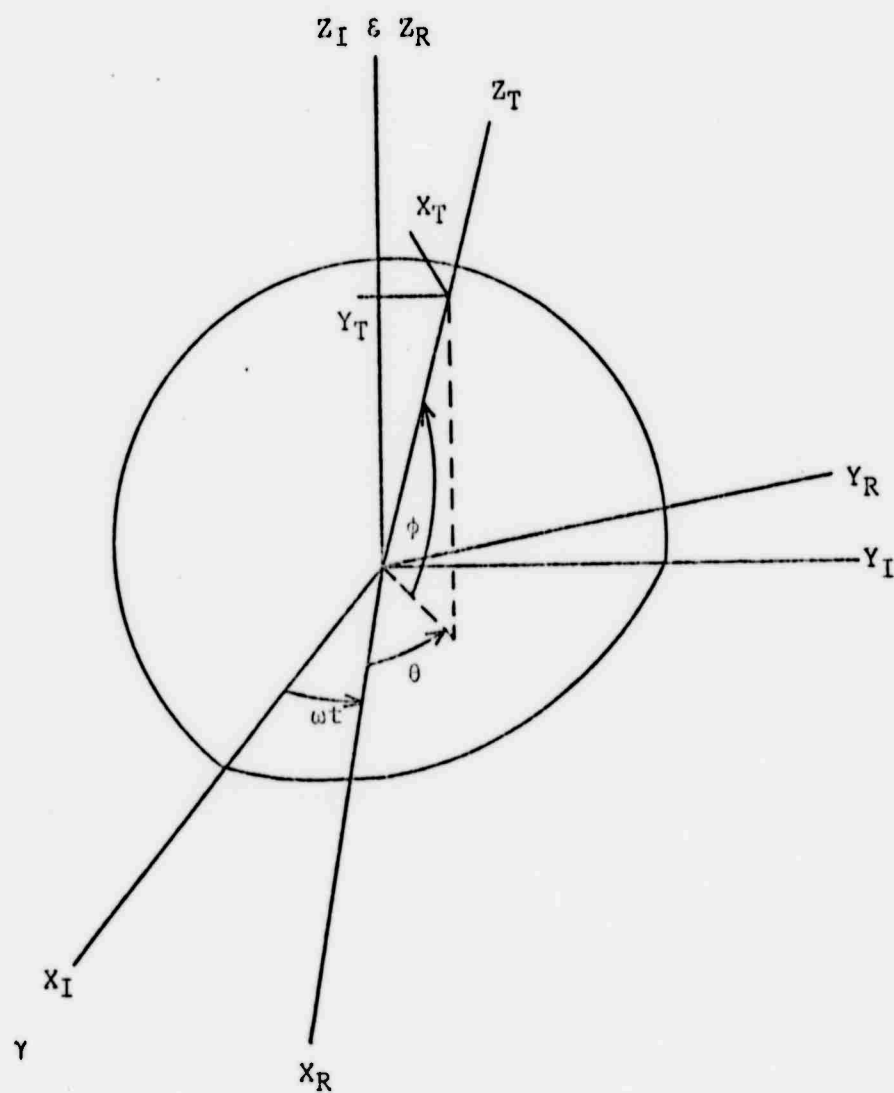
Figure 1. Earth Centered Inertial and Rotating and Station Centered Topocentric Coordinate Systems

the station. The Z_T axis is straight up from the station, while the Y_T axis is toward local West in the tangent plane. The actual and computed values of the measurements are expressed in this frame.

Coordinate Transformations

Transformations between any two reference systems are readily made with two matrices: the transformation matrix between the inertial and rotating geocentric frames, and the transformation matrix between the rotating geocentric and topocentric frames. The matrices are given below with the angles as shown in Figure 1.

$$
\begin{bmatrix} x_T \\ y_T \\ z_T \end{bmatrix} = \begin{bmatrix} -\sin(\phi)\cos(\theta) & -\sin(\phi)\sin(\theta) & \cos(\phi) \\ \sin(\theta) & -\cos(\theta) & 0 \\ \cos(\phi)\cos(\theta) & \cos(\phi)\sin(\theta) & \sin(\phi) \end{bmatrix} \begin{bmatrix} x_R \\ y_R \\ z_R \end{bmatrix} \qquad (1)
$$

$$
\begin{bmatrix} x_R \\ y_R \\ z_R \end{bmatrix} = \begin{bmatrix} \cos(\omega t) & \sin(\omega t) & 0 \\ -\sin(\omega t) & \cos(\omega t) & 0 \\ 0 & 0 & 1 \end{bmatrix} \begin{bmatrix} x_I \\ y_I \\ z_I \end{bmatrix} \qquad (2)
$$

Since these are orthogonal transformations, any other necessary relationships may be determined by multiplying and/or transposing these two matrices.

Equations of Motion

The equations of motion of a satellite about a spherical earth are a set of three second order non-linear differential equations. In inertial coordinates they are

7

$$\ddot{x}_I = \frac{-\mu x_I}{r^3} \tag{3}$$

$$\ddot{y}_I = \frac{-\mu y_I}{r^3} \tag{4}$$

$$\ddot{z}_I = \frac{-\mu z_I}{r^3} \tag{5}$$

while in earth-centered rotating coordinates they are

$$\ddot{x}_R = \frac{-\mu x_R}{r^3} + 2\omega\dot{y}_R + \omega^2 x_R \tag{6}$$

$$\ddot{y}_R = \frac{-\mu y_R}{r^3} - 2\omega\dot{x}_R + \omega^2 y_R \tag{7}$$

$$\ddot{z}_R = \frac{-\mu z_R}{r^3} \tag{8}$$

These second order equations can be reduced to first order equations by the use of a state vector formulation. The state vector, $\underline{x}$, is defined as

$$
\begin{array}{ll}
x_1 = x & x_4 = \dot{x} \\
\\
x_2 = y & x_5 = \dot{y} \\
\\
x_3 = z & x_6 = \dot{z}
\end{array}
\tag{9}
$$

The equations of motion then become the 6×1 vector differential equation

$$\underline{\dot{x}}(t) = \underline{f}(\underline{x}(t)) \tag{10}$$

8

where $\underline{f}$ is a 6×1 vector valued function. In inertial coordinates the state differential equation is

$$\underline{\dot{x}}_I(t) = \underline{f}_I(\underline{x}_I(t)) = \begin{bmatrix} x_4 \\[1em] x_5 \\[1em] x_6 \\[1em] \dfrac{-\mu x_1}{r^3} \\[1em] \dfrac{-\mu x_2}{r^3} \\[1em] \dfrac{-\mu x_3}{r^3} \end{bmatrix} \tag{11}$$

and in rotating coordinates the state differential equation is

$$\underline{\dot{x}}_R(t) = \underline{f}_R(\underline{x}_R(t)) = \begin{bmatrix} x_4 \\[1em] x_5 \\[1em] x_6 \\[1em] \dfrac{-\mu x_1}{r^3} + 2\omega x_5 + \omega^2 x_1 \\[1em] \dfrac{-\mu x_2}{r^3} - 2\omega x_4 + \omega^2 x_2 \\[1em] \dfrac{-\mu x_3}{r^3} \end{bmatrix} \tag{12}$$

9

Initial Conditions

In applying WLS and the Kalman filter to the orbit problem, an initial or nominal state vector must be available. Since the early-orbit determination problem is very important in non-nominal launches, it was decided to determine the initial state from the first set of input data rather than use a nominal vector. This data set includes range, range rate, azimuth, elevation, azimuth rate, and elevation rate. The angular rates are needed to complete the set of six independent constants for the equations of motion. The initial position and velocity vectors in the rotating coordinate system are then determined by the vector equations below and the exact method (Ref 3:88-90) is presented in Appendix A.

$$\underline{r} = \rho\underline{L} + \underline{R} \tag{13}$$

$$\underline{\dot{r}} = \dot{\rho}\underline{L} + \rho\underline{\dot{L}} \tag{14}$$

This initial state vector is then transformed to an inertial vector for use in the WLS program.

Data Generation

To generate noisy data for the two orbit determination schemes, the inertial equations of motion are integrated through the desired time interval with the starting position and velocity chosen from a desired nominal orbit. As the satellite passes over the hypothetical station location, nominal tracking data is produced via a coordinate transformation from inertial to rotating geocentric and topocentric coordinates. Once x_R, y_R, z_R, $\dot{x}_R$, $\dot{y}_R$, $\dot{z}_R$, x_T, y_T, and z_T are known, the nominal observation data are determined by

10

$$\rho = [(x_R-x_S)^2 + (y_R-y_S)^2 + (z_R-z_S)^2]^{1/2} \tag{15}$$

$$\dot{\rho} = \frac{1}{\rho} [(x_R-x_S)\dot{x}_R + (y_R-y_S)\dot{y}_R + (z_R-z_S)\dot{z}_R] \tag{16}$$

$$a = \tan^{-1} [-y_T/x_T] \tag{17}$$

$$e = \tan^{-1} [z_T/(x_T^2 + y_T^2)^{1/2}] \tag{18}$$

where x_S, y_S, and z_S are the station coordinates in the rotating geocentric system. If the elevation is above a threshold value, the observation data are stored along with time from t_0. When the integration has reached t_f, the table of observations is contaminated by zero-mean Gaussian noise.

The random number generator on the CDC 6600 produces a uniform random number sequence between 0 and 1, thus the mean of this sequence is 0.5 and the variance is 1/12. To convert this sequence to an approximate normal sequence of mean zero and variance one, the Central Limit Theorem is used. This theorem applied to a uniform sequence states that

$$\lim_{n \to \infty} \left(\frac{S_n - n\mu}{\sigma \sqrt{n}} \right) = N(0,1) \tag{19}$$

where S_n is the sum of n uniform numbers, μ is the uniform mean, σ is the uniform standard deviation, and N is the normal distribution function. In n=12, the equation reduces to

11

$$\sum_{i=1}^{12} x_i - 6 = N(0,1) \qquad (20)$$

and a normal distribution curve is approximated by a 12th order
polynomial. This is the equation used to produce the approximate
zero-mean Gaussian sequence. To change the variance, each random
number is multiplied by the desired standard deviation, producing a
$N(0,\sigma^2)$ distribution. If started at the same place, this random
number generator will always generate the same sequence realization;
thus, to obtain different realizations the generator is started with
a random initial condition. This normal distribution approximation
suffers from one disadvantage in that only a 6σ range is produced,
thus the "tails" of the curve are not generated. The impact of this
on the orbit problem is that very large data errors are not encountered
and the filters may perform better than they would with normally
distributed data.

III. The Kalman Filter Equations

Measurement Model

The Kalman filter as described in Reference 4 processes noisy linear data in a recursive manner to produce a linear unbiased minimum variance estimate of the state of a linear dynamic system. The data consist of a linear function of the state plus additive Gaussian noise.

In the orbit determination problem, the data are ground radar measurements range (ρ), range rate ($\dot\rho$), azimuth (a), and elevation (e) which, as seen in equations (15-18) are not linearly related to the state vector and the station position vector. The measurement model may be expressed as a discrete non-linear vector equation

$$\underline{z}(k) = \underline{h}[\underline{x}(k)] + \underline{v}(k) \tag{21}$$

where $\underline{z}$ is a 4×1 vector consisting of ρ, $\dot\rho$, a, and e; $\underline{h}$ is a non-linear vector valued function; and $\underline{v}$ is a white Gaussian sequence. It is assumed that the noise has mean

$$E[\underline{v}(k)] = 0 \tag{22}$$

in this case but this assumption is not necessary in the general problem. The noise covariance is assumed to be

$$E[\underline{v}(k)\underline{v}^T(k)] = R(k)\,\delta_{ij} \tag{23}$$

where $R(k)$ is a known positive semi-definite matrix.

Filter Equations

Since the Kalman filter assumes a linear system and a linear measurement model, the filter cannot be applied directly to estimating the state of a satellite orbit based on a sequence of noisy radar observations. Equations (12) and (21) are the non-linear state and measurement equations and must be approximated by a linearized set of equations before the linear filter can be used. The two sets of equations are expanded in a Taylor series about a suitable point and first-order terms are retained. The linearized equations are

$$\underline{\dot{x}}(t) = F\underline{x}(t) \tag{24}$$

and

$$\underline{z}(k) = M\underline{x}(k) + \underline{v}(k) \tag{25}$$

where F is the 6×6 State Sensitivity Matrix

$$F(\underline{x}) = \left.\frac{\partial \underline{f}(\underline{x})}{\partial \underline{x}}\right|_{\underline{x} = \underline{\hat{x}}(k+1|k)} \tag{26}$$

and M is the 4×6 Measurement Matrix

$$M(\underline{x}) = \left.\frac{\partial h(\underline{x})}{\partial \underline{x}}\right|_{\underline{x} = \underline{\hat{x}}(k+1|k)} \tag{27}$$

The exact form of these matrices is developed in Appendices B and C.

The nominal point about which the non-linear equations are expanded is the current state estimate $\underline{\hat{x}}$ based on the previous measurement at time k and integrated forward via equation (12) to time k+1. As a result of updating the nominal at each time point, initial errors

14

are not allowed to propagate through time and the linearity assumptions should be more valid as the filter progresses (Ref 4:276).

Now that the state and measurement equations are in a linear form, the recursive Kalman filter equations can be applied. The filter consists of a predictor in which the estimated state and state error covariance are integrated forward to the next observation time point and a corrector in which the state estimate and estimated state error covariance are corrected by the new observation data.

Prediction. Prediction from time t_k to time t_{k+1} is accomplished by numerically integrating the state vector differential equation (12). In discrete form this equation becomes

$$\underline{\hat{x}}(k+1|k) = \underline{\hat{x}}(k|k) + \int_{t_k}^{t_{k+1}} \underline{f}[\underline{\hat{x}}(k|k)]dt \tag{28}$$

The state error covariance at time t_{k+1} based on data at time t_k is

$$P(k+1|k) = \Phi(k+1,k)P(k|k)\Phi^T(k+1,k) \tag{29}$$

where $\Phi(k+1,k)$ is the State Transition Matrix:

$$\Phi(k+1,k) = \frac{\partial\underline{\hat{x}}(k+1)}{\partial\underline{\hat{x}}(k)} \tag{30}$$

$\Phi(k+1,k)$ is determined by integrating the linear differential matrix equation

$$\dot{\Phi}(k+1,k) = F[\underline{\hat{x}}(k|k)]\Phi(k+1,k) \tag{31}$$

$$R = \begin{bmatrix} \sigma_\rho^2 & & & 0 \\ & \sigma_\rho^2 & & \\ & & \sigma_\rho^2 & \\ 0 & & & \sigma_\rho^2 \end{bmatrix} \qquad (38)$$

The error covariance of the corrected state estimate, $\underline{\hat{x}}(k+1|k+1)$, is determined by the equation

$$P(k+1|k+1) = [I-K(k+1)M]P(k+1|k)[I-K(k+1)M]^T +$$
$$K(k+1)RK(k+1)^T \qquad (39)$$

where M is again calculated at time t_{k+1}.

To start the process, values of $\underline{\hat{x}}(0|0)$, $P(0|0)$, and R must be available. The initial state estimate, $\underline{\hat{x}}(0|0)$, is computed by the method in Chapter II; the initial state error covariance matrix, $P(0|0)$, must be estimated a priori; and the measurement error covariance matrix, R, is known from antenna tests, or, when the input data are simulated, from the variances of the noise added to the measurements.

The filter used in this manner is referred to as the Extended Kalman filter due to the fact that the equations are linearized about the current state estimate, $\underline{\hat{x}}(k+1|k)$. The prediction process does not involve any linear assumptions, as the non-linear equations (12) and (33) are used to predict the state and the measurement and the state error covariance is predicted by the linear matrix differential equation (29). The linearization procedure is only used in the calculation of the corrected state estimate and corrected state error

17

covariance, i.e., linearization involves the state errors rather than the states themselves.

A derivation of the Extended Kalman filter is found in Reference 4 and a flow diagram for the filter is presented in Figure 2.
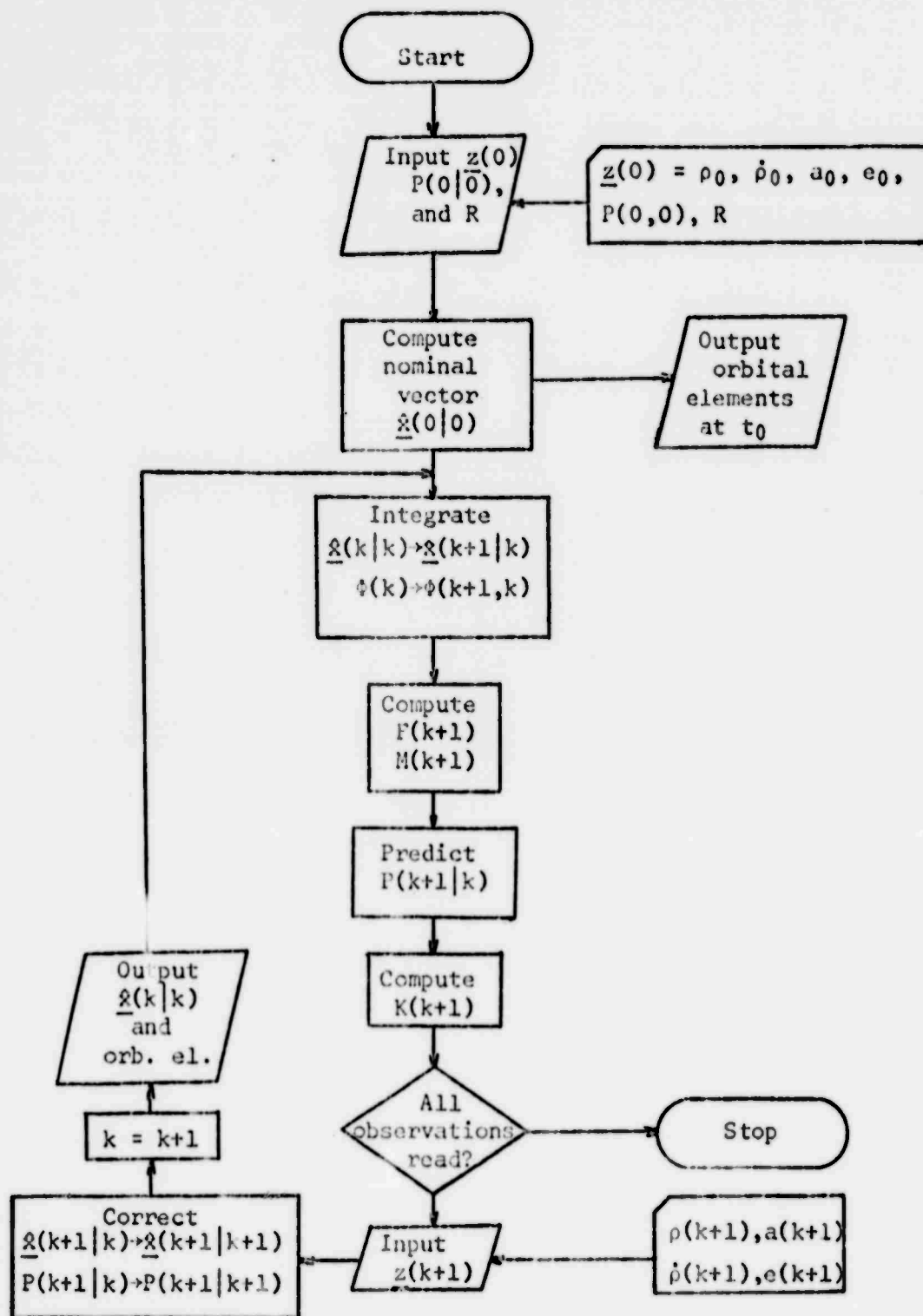
Figure 2. Extended Kalman Filter Flowchart

IV. Weighted Least Squares

Least Squares Theory

The goal of the method of Weighted Least Squares when applied to orbit determination is to determine the values of the six orbit parameters at some epoch time, t_0, given sets of observation data such that the cost function

$$J = ||\underline{y} - \underline{\hat{y}}(\underline{\hat{x}}_0)||_W^2 = [\underline{y} - \underline{\hat{y}}(\underline{\hat{x}}_0)]^T W[\underline{y} - \underline{\hat{y}}(\underline{\hat{x}}_0)] \tag{40}$$

is a minimum. W is an appropriate weighting matrix; $\underline{y}$ is the observation vector consisting of range, range rate, azimuth, and elevation at each discrete time t_k, $(t_0 \leq t_k \leq t_f)$, and $\underline{\hat{y}}$ is the predicted observation vector based on the current state vector estimate $\underline{\hat{x}}$ at t_0. Thus $\underline{y}$ is the 4n×1 measurement vector

$$\underline{y} = \begin{bmatrix} \underline{z}t_0 \\ \underline{z}t_1 \\ \underline{z}t_2 \\ \cdot \\ \cdot \\ \cdot \\ \underline{z}t_f \end{bmatrix} \tag{41}$$

and $\underline{\hat{y}}$ is the 4n×1 estimated measurement vector

$$\hat{\underline{y}} = \begin{bmatrix} \underline{\hat{z}}_1 \\ \underline{\hat{z}}_2 \\ \underline{\hat{z}}_3 \\ \cdot \\ \cdot \\ \cdot \\ \underline{\hat{z}}_n \end{bmatrix} \tag{42}$$

The value of $\underline{x}_0$ which minimizes the cost function is the "best" estimate in the least squares sense.

Since the predicted observation vector $\hat{\underline{y}}$ is a non-linear function of the states, the equation relating them must be linearized by expanding $\hat{\underline{y}}$ in a Taylor series about $\underline{\hat{x}}_0$ and dropping higher order terms. The cost function becomes

$$J = ||\Delta\underline{y}||^2_W = ||\Lambda\underline{y} - \Lambda\Lambda\underline{x}_0||^2_W \tag{43}$$

where A is the $4n\times6$ Measurement Sensitivity Matrix

$$\Lambda = \frac{\partial\hat{\underline{y}}}{\partial\underline{x}}\bigg|_{\underline{x} = \underline{\hat{x}}_0} \tag{44}$$

and

$$\Delta\underline{y} = \underline{y} - \hat{\underline{y}}(\underline{\hat{x}}_0) \tag{45}$$

21

Differentiating equation (43) with respect to the state correction vector, $\Delta \underline{x}_0$, and setting the result equal to zero:

$$2[A^T W A \Delta \underline{x}_0 - A^T W \Delta \underline{y}]^T = 0 \tag{46}$$

This equation is then solved for $\Delta \underline{x}_0$, yielding the normal matrix equation for the WLS problem:

$$A^T W A \Delta \underline{x}_0 = A^T W \Delta \underline{y} \cdot \tag{47}$$

or

$$\Delta \underline{x}_0 = [A^T W A]^{-1} A^T W \Delta \underline{y} \tag{48}$$

The differences, $\Delta \underline{y}$, are the residuals of the measurements and are the result of the random observation noise, incorrect values of the estimated state $\hat{\underline{x}}_0$, and computation errors. Since the original WLS problem has been reduced to the linearized problem of determining a correction vector $\Delta \underline{x}_0$ such that

$$|| \Delta \underline{y} - A \Delta \underline{x}_0 ||_W^2 \tag{49}$$

is minimized, the solution is only approximate. Therefore, an iterative process must be used until the residuals are reduced to some minimum (Ref 7:2-4).

Convergence Criteria

In order to determine when to stop the iteration process, some convergence criteria must be employed. Using the corrected state vector to predict a new set of weighted residuals

22

$$||\Delta \underline{y}^P||_W^2 = ||\Delta \underline{y} - A\Lambda \underline{x}_0||_W^2 \qquad (50)$$

The expression $||\Delta \underline{y}^P||_W$ is then the RMS of the predicted residuals. The least squares process is said to converge if either

$$\frac{||\Delta \underline{y}||_W - ||\Delta \underline{y}^P||_W}{||\Delta \underline{y}||_W} \leq \varepsilon_1 \qquad (51)$$

or

$$||\Delta \underline{y}||_W - ||\Delta \underline{y}^P||_W \leq \varepsilon_2 \qquad (52)$$

where $||\Delta \underline{y}||_W$ is the RMS of the current weighted residuals and ε_1 and ε_2 are some small constants (Ref 7:20). The values chosen for ε_1 and ε_2 for this study were both 2×10^{-4}.

Sensitivity Matrix

The Measurement Sensitivity Matrix, A, may be calculated using the chain rule:

$$A = \frac{\partial \hat{\underline{y}}}{\partial \underline{x}_0} = \frac{\partial \hat{\underline{y}}}{\partial \underline{x}_t} \frac{\partial \underline{x}_t}{\partial \underline{x}_0} \qquad (53)$$

and defining

$$M = \left. \frac{\partial \underline{z}_t}{\partial \underline{x}_t} \right|_{\underline{x}^h} \qquad (54)$$

23

the 4×6 Measurement Matrix, and

$$\phi(t,t_0) = \frac{\partial \underline{x}_t}{\partial \underline{x}_0} \tag{55}$$

the 6×6 State Transition Matrix. The State Transition Matrix is computed by integrating the matrix differential equation

$$\dot{\phi}(t,t_0) = F\phi(t,t_0) \tag{56}$$

with initial conditions

$$\phi(t_0,t_0) = I \tag{57}$$

where

$$F = \left. \frac{\partial f(x)}{\partial \underline{x}} \right|_{\underline{x}^*} \tag{58}$$

and the nominal point $\underline{x}^*$ used in equations (54) and (58) is on the trajectory predicted by the current value of $\underline{x}_0$. Since the M and F matrices are calculated at each observation point in the trajectory, the A matrix actually consists of the partitioned matrix

$$A = \begin{bmatrix} M_0\phi(t_0,t_0) \\ M_1\phi(t_1,t_0) \\ \cdot \\ \cdot \\ \cdot \\ M_n\phi(t_n,t_0) \end{bmatrix}_{4n\times6} \tag{59}$$

The derviation of the F and M matrices is in Appendices B and C.

24

Statistical Aspects

Until now, nothing has been said about either statistical theory or the contents of the weighting matrix, W. For many years, this matrix was guessed for each problem and was used as a "fudge factor" since it seemed reasonable to weight "reliable" data more heavily than "unreliable" data. However, recent statistical theory shows that if this weighting matrix is chosen to be the inverse of the observation error covariance, R, and the observation errors have a zero-mean, then the matrix

$$P = A^T W A = A^T R^{-1} A \tag{60}$$

is the state error covariance matrix. In addition, the estimated state error, $\Delta \underline{x}_0$, which results from equation (48) using the covariance matrix, P, is the linear unbiased minimum variance estimate of the state error. If the observation errors have a joint Gaussian distribution, then the state error estimate is also the maximum likelihood estimate (Ref 7:25-26).

Computational Procedure

The procedure used to determine the satellite's orbit parameters using WLS are as follows:

1. Set $A = \phi$. Input R and $\underline{z}_0$ where $\underline{z}_0$ consists of ρ, $\dot{\rho}$, a, and e.

2. Determine an initial nominal state vector, $\underline{\hat{x}}_0$, from the first data set (ρ, $\dot{\rho}$, a, e, $\dot{a}$, and $\dot{e}$).

3. Integrate the trajectory and the State Transition Matrix from t_0 to t_f.

(a) At each time point, t_k, calculate and store

$$\hat{\underline{y}}_k = \underline{2}(\underline{\hat{x}}_0) \tag{61}$$

the predicted measurement

$$M_k, \text{ the Measurement Matrix} \tag{62}$$

$$A_k = A_{k-1} + M_k \Phi(t_k, t_0) \tag{63}$$

and

$$\Delta \underline{y}_k = \underline{z}_k - \underline{2}(\underline{\hat{x}}_0)_k \tag{64}$$

the measurement residual.

4. When $t = t_f$, calculate

$$P = A^T R^{-1} A \tag{65}$$

the state error covariance, and

$$||\Delta \underline{y}||_W \tag{66}$$

the weighted residual vector RMS.

5. Invert the covariance matrix and calculate

$$\Delta \underline{x}_0 = P^{-1} A^T R^{-1} \Delta \underline{y} \tag{67}$$

then

$$\underline{\hat{x}}_0 = \underline{\hat{x}}_0 + \Delta \underline{x}_0 \tag{68}$$

26

6. Calculate the predicted RMS

$$||\Delta\underline{y}^P||_W = [||\Delta\underline{y} - A\Delta\underline{x}_0||_W]^{1/2} \qquad (69)$$

and determine whether or not the convergence criteria have been met. If they have not, return to step 3 with the new $\underline{x}_0$. If the convergence criteria have been met, stop. If the predicted RMS is greater than the current RMS, or if the current RMS is greater than the old RMS, the process is diverging, indicating some problem with either the data or the system model. In this case, the process stops and all of the data must be examined. One type of data which can cause divergence is an "outlier"--a data point very far from the other points. This point can be spotted by looking at the residuals of the measurements and must be manually thrown out. The WLS procedure would then be restarted without the outliers.

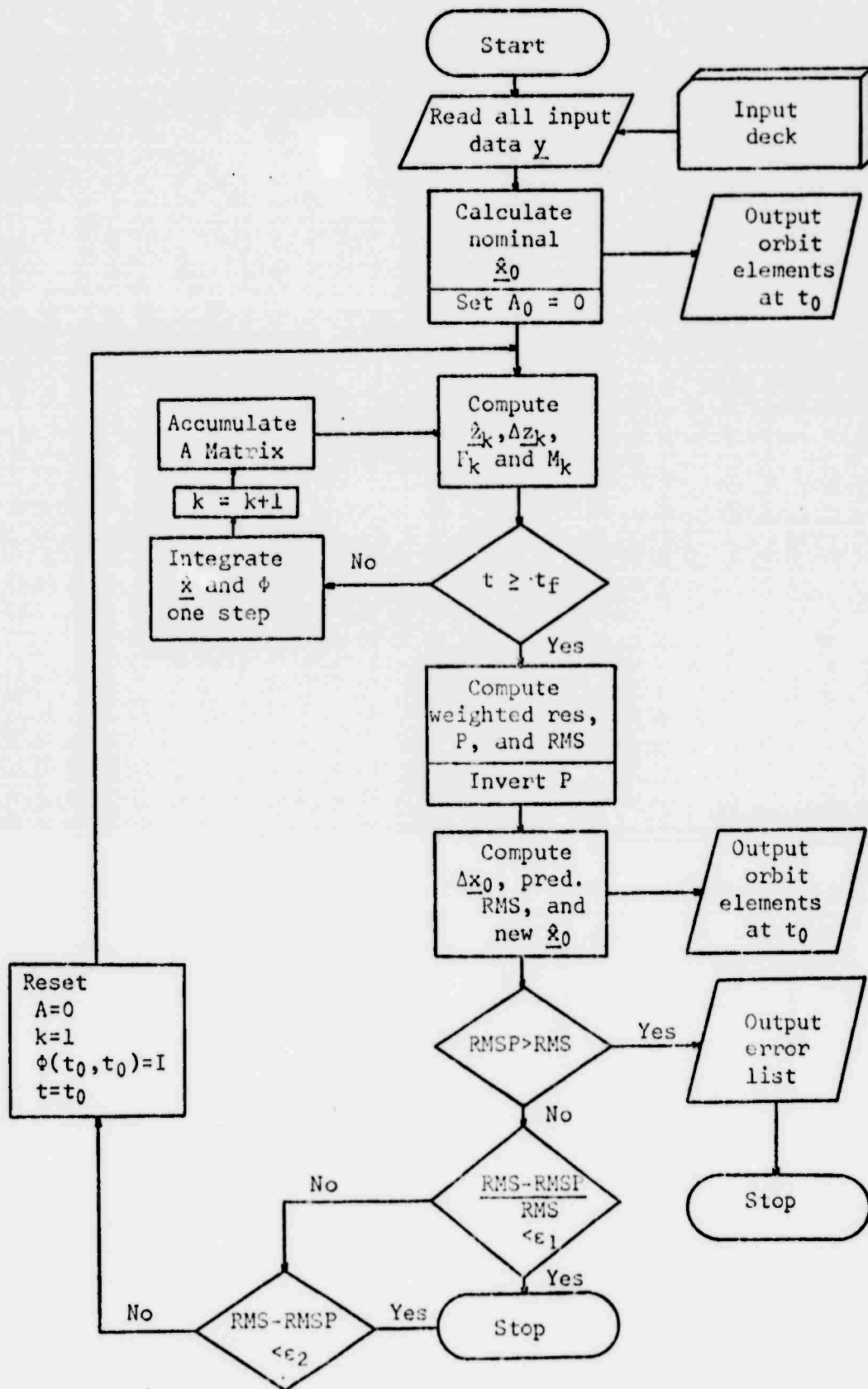A computer flowchart for the WLS method is shown in Figure 3.

Figure 3. Weighted Least Squares Filter Flowchart

V. Comparison of the Operation of th Two Filters

Theory of the Two Methods

It was stated in Chapters III and IV and shown in References 4 and 7 that both of the methods produce a linear unbiased minimum variance estimate of the state of a linear system given linear measurements with additive noise. Reference 7 (page 157) lists a number of authors who have shown that when the Weighted Least Squares method is applied in a recursive manner, the resulting equations are exactly the same as those in the Kalman filter. Therefore, the only difference between the two methods compared in this paper is that one is a batch processor while the other is recursive. Both are linear processors and both linearize the earrors in the orbit problem. The Extended Kalman filter linearizes about the current state estimate at time t_K, while WLS linearizes about the state estimate at t_0.

Advantages and Disadvantages

Since the two methods are of the same form, the only theoretical comparisons which can be made are those between batch and recursive processing. The following are a few of the theoretical advantages and disadvantages of the Extended Kalman filter as compared with the method of Weighted Least Squares.

A. Since the filter linearizes about the current state, a large initial error plus many observations over a long time span would probably not cause the filter to diverge while WLS may diverge. This is because WLS would use the erroneous initial orbit to predict for the entire span and errors at later times may be so large that the linearity assumptions are violated.

B. With a large amount of data, both methods tend to ignore changes in new data. In WLS, the new data are overcome by the preponderance of older data and in the filter, once it "learns" the model, the Kalman gain becomes so small that new data are under-weighted. The solution in both cases is to restart the process and leave out most of the old data.

C. The filter data storage is small while the WLS residual vector must be stored and may be very large.

D. The filter processing requirements are quite a bit larger than the requirements of WLS.

E. As stated in Reference 1 (page 390), the filter processor is slower than one iteration of WLS, however, WLS usually requires more than one iteration, so they both require similar central processor time.

F. The filter produces an estimate of the state, the state error, and the state error covariance at each point in the process. The estimated error and error covariance are extremely useful in analysis of the process as any outliers in the data are very apparent, so that real-time control of the data is possible. The WLS method gives a weighted RMS and predicted RMS in addition to the state error covari-ance, but these only give an indication of what the processor did after an iteration. The whole residual vector must be examined to discover outliers, and, if the process diverged, there is usually no clear reason for the problem, nor is there shown any time point at which the process started to blow up.

This time history output of the filter is probably the most important advantage compared to WLS. It can be used to determine the exact time at which a problem occurs, and if the process starts to diverge at any point, it may be restarted after that point with only the initial guess of $P(k|k)$ and $\hat{x}(k)$ needed.

VI. Results

In order to compare the performance of the two filters in the early-orbit determination problem, noisy observations produced by the generation program and necessary station data are input to the two filtering programs. The comparison then consists of two parts. First, to compare the application of the two methods to this problem, a single pass of observation data is processed by each program. The same data set is input to each computer program so that the results can be compared. The resulting outputs of the two filters are then compared to determine their suitability to the orbit determination problem and to show the type of information they each provide. The filters are rerun for varying numbers of observations so that the effects of observation truncation may be seen.

Next, to obtain a comparison of the two filters' absolute accuracies, their radial and velocity estimates for various numbers of observations are compared to the actual orbit radii and velocities. This provides an absolute accuracy comparison of the two methods.

If only one set of observations were used in making this absolute comparison, the results would not be valid. This is because the observation sequence is finite and the additive noise is a truncation of an infinite noise sequence which has Gaussian statistics. Therefore, the statistics of any single truncated realization of the infinite sequence will probably not have the desired Gaussian statistics. A reasonable approximation to the Gaussian statistics on the additive noise is obtained by taking an ensemble average of the filters' outputs for 50 different truncated random sequences used for the additive
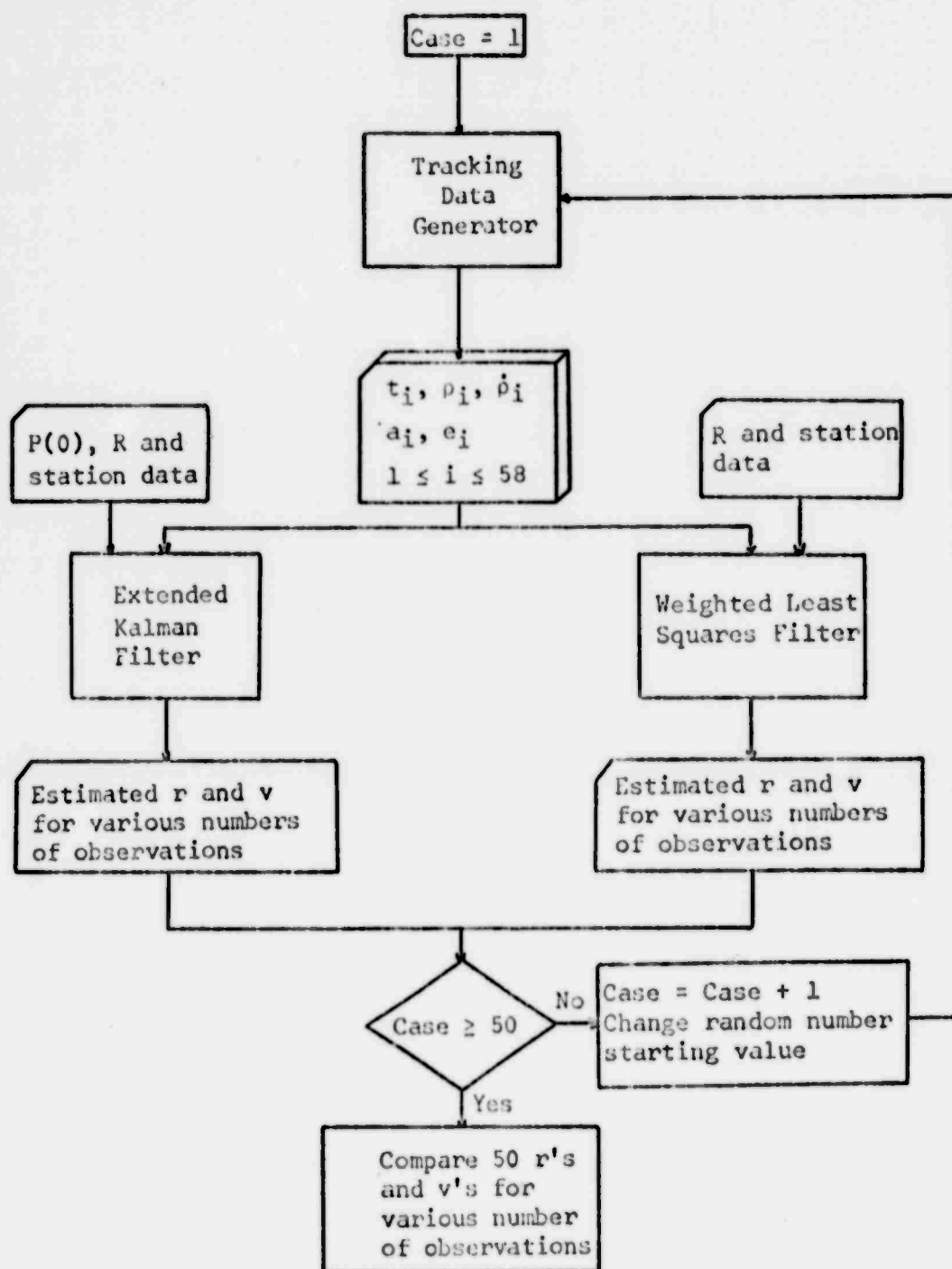
Figure 4. Observation Data Generation and Filter
Accuracy Comparison Flowchart

noise. The results to be compared are then the mean radial and velocity errors of the 50 runs. Figure 4 shows a flow diagram of the accuracy comparison process. Fifty data sets of 58 observations each are produced, radial and velocity vectors are estimated by the two filters and the magnitudes of these vectors are compared with their actual values from the nominal orbit.

Data

The actual orbit parameters of the two-body orbit are given in Table I along with the location of the hypothetical tracking station and the sigmas of the noisy observations. A medium-altitude orbit was chosen because atmospheric drag and solar pressure are small in this region and the assumptions of a two-body problem with no drag would be more realistic.

Since the problem is an early-orbit problem, only one tracking pass was used. This particular data set simulates a near-polar satellite launched at Vandenberg Air Force Base passing over Shemya Tracking Station on the first orbit.

Filter Output Comparison

Table II shows the error magnitudes predicted by the Kalman filter, the standard deviations predicted by each of the methods and the actual radial and velocity error magnitudes for a various number of observations. Since these estimated values are for only one pass of data which ranged from 4 to 58 observations, the actual numbers give an indication of the order of magnitude of the outputs of the two programs. The main result of this comparison lies in the trends

Table I

Actual Orbit and Sensor Data

True Two-Body Keplerian Orbit Parameters		
Period	Inclination	Eccentricity
96.38295 Min	56.0713 Deg	0.00312689
Longitude of Ascending Node	Argument of Perigee	Perigee Height
203.3325 Deg	218.1018 Deg	304.2986 NM
Radius at t_0	Velocity at t_0	
6983973.2 M	7543.61 M/S	

Tracking Station Sensor Data			
Latitude		Longitude	Height
52.73267 N		174.1023 E	0.0
Azimuth Sigma (Deg)	Elevation Sigma (Deg)	Range Sigma (M)	Range Rate Sigma (M/S)
0.02	0.02	100.0	1.0

Table II

Kalman and Least Squares Radial and Velocity Errors - Single Run

Number of Points	Kalman Filter						Least Squares			
	Estimated Error		Estimated Error Sigma		Actual Error		Estimated Error Sigma		Actual Error	
	Radial (M)	Velocity (M/S)	Radial (M)	Velocity (M/S)	Radial (M)	Velocity (M/s)	Radial (M)	Velocity (M/s)	Radial (M)	Velocity (M/S)
4	238.5	17.3	346.4	26.95	410.3	3.92	368.0	16.04	215.0	1.85
8	203.6	5.44	248.3	9.25	16.0	0.40	272.5	9.29	58.3	2.19
10	56.4	1.22	219.3	6.53	28.1	1.24	244.9	6.31	12.9	0.53
20	109.5	1.34	150.9	2.26	80.3	0.98	171.4	2.29	13.2	0.57
30	15.0	0.12	132.2	1.29	42.0	0.36	140.2	1.29	19.9	0.14
40	16.3	0.09	133.3	0.93	8.7	0.28	123.2	0.86	46.1	0.08
50	25.9	0.13	141.4	0.74	29.0	0.17	112.5	0.74	44.0	0.02
58	17.5	0.06	149.5	0.65	8.3	0.05	106.4	0.65	21.6	0.05

of the errors and standard deviations as the number of observations
is varied.

As seen in Table II, the estimated sigmas produced by each method
are fairly close but the Least Squares radial and velocity sigmas
decrease monotonically, while the Kalman filter's radial sigma reaches
a low at around 30 tracking points and then starts climbing slowly.
This is probably due to the accumulation of computer round-off error.
Since the Kalman filter computes the covariance matrix in a recursive
manner, any errors will be additive and will finally affect the
significant digits of the estimates covariance and, subsequently, of
the estimated state. Since the radial variance is so much larger than
the velocity variance, this effect would be observed first in the
radial sigma, as seen in Table II. The WLS process computes the
estimated state and state covariance independently from one iteration
to the next, so round-off errors cannot propagate from one calculation
to the next. Thus the radial and velocity sigmas produced by this
filter do not show any growth.

The estimated state error produced by the filter has no counter-
part in WLS. Since WLS does all of its state calculations at t_0, no
time history of state errors is generated. As seen in Table II, these
estimated error values are not close to the actual errors in most
cases but they do give an indication of the order of magnitude of the
actual errors and of the stability of the process. Whenever the
estimated error is greater than the estimated sigma a majority of the
time the filter is diverging. When these values are plotted, as in
Figures 5 and 6, they give a good picture of the operation of the

filter. This is the "big picture" which WLS cannot produce. Figures 5 and 6 show that the filter has no tendencies toward divergence in this case. No divergent examples occurred in this study, and none were expected since the model and the actual system were the same non-linear system of equations. In addition, the noisy data used in this problem were reasonably well-behaved since they contained no additive noise larger than six sigma. In a real situation, a pre-processor would be used to remove extremely noisy data, so the results of this study should be applicable to real systems where the actual model is known fairly well.

Orbit Parameters. When an early-orbit determination program is actually used, the program's output which has physical significance is not the radius or velocity but the orbit parameters. Thus, to compare the two filters' application to this problem requires a comparison of the estimated orbit parameters with the actual parameters.

Table III shows the orbit parameters computed from the estimated radius and velocity produced by each method from various numbers of observations. The method of calculating the two-body orbit parameters from radius and velocity is given in Reference 2 (pages 98-107). Even with as few as ten observations, the predicted orbit parameters are fairly close to the actual values, and with the whole pass the errors are extremely small.

The most important element to be computed in the early-orbit situation is the period. This is because the pointing data at the next station are very sensitive to period errors. A period change of only 10 seconds could cause the satellite to be outside the beam width of

Table III

Actual, Kalman and Least Squares Orbit Parameters - Single Run

Parameter	Actual Value	Kalman Filter		Least Squares	
		10 Pts	58 Pts	10 Pts	58 Pts
Period (Min)	96.33295	96.33439	96.33052	96.40228	96.33333
Error (Sec)		2.85	0.14	1.16	0.02
Eccentricity	0.0031269	0.0034935	0.0031391	0.0029847	0.0031171
Error		0.0002666	0.0000122	0.0001422	0.0000098
Inclination (Deg)	56.0713	56.0650	56.0702	56.0678	56.0704
Error (Deg)		0.0063	0.0011	0.0035	0.0009
Longitude of Ascending Node (Deg)	203.3325	203.3186	203.3301	203.3242	203.3306
Error (Deg)		0.0139	0.0024	0.0056	0.0005
Argument of Perigee (Deg)	218.1018	217.9550	218.2712	217.9847	218.2906
Error (Deg)		0.1468	0.1694	0.0297	0.0194

the tracking antenna. The period is a simple function of the radius and velocity, as seen from the following equations.

$$\text{period (seconds)} = \frac{2\pi a^{3/2}}{k\sqrt{\mu}} \qquad (70)$$

where

$$a = \frac{\mu r}{2 - rv^2} \qquad (71)$$

and k is the Earth gravitation constant in radians/second. Thus the sensitivity of the period to errors in radius and velocity is a direct function of errors in each one. As seen in Table III, the period estimated by each filter using 58 observations is much less than one second from the true value, hence the satellite should be easy to find at the second and subsequent stations.

Accuracy Comparison Using 50 Data Sets

Figures 7 and 8 show the two filters' mean radial and velocity error for 50 runs versus the number of observations while Figures 9 and 10 show the radial and velocity error standard deviations. The errors are defined as estimated minus actual values. Figure 9 shows that the Kalman filter has a slightly smaller radial error sigma when less than 30 observations are processed, while WLS appears slightly better for data amounts greater than that threshold. This appears consistent with the theory since the Kalman filter "learns" the model faster than the WLS filter, but once the Kalman filter errors reach a minimum, the covariance error starts growing and affects the estimate

accuracy. WLS does not experience the covariance error so the actual errors continue to decrease with the number of observations processed.

Figure 10 shows that the velocity error distributions of both methods are so similar that they are indistinguishable. Since the velocity magnitudes are so much smaller than the radial magnitudes, the difference in the errors in velocity are not as noticeable as the radial errors.

Non-Linearity Problems. Figures 7 and 8 reveal a problem with the Kalman filter. The estimates of the two methods should be unbiased, however the Kalman filter's mean radial and velocity errors show a small negative bias after some rather large initial errors. This bias of approximately 30 meters in radius represents an error of 0.0005% and the velocity bias of approximately 0.1 m/s is an error of 0.001%, so it would never be apparent when one case is run at a time. Only when several cases were studied did the small biases become apparent. The effect of errors of these magnitudes is seen in Table III in which the velocity and radial errors for 58 observations are nearly the same as the mean errors of the 50 runs.

In the search for some bias in the computer program, it was found that the initial velocity estimated by the initial condition module was always 500 to 700 m/s higher than the actual velocity. This large velocity error is nearly 10% of the actual velocity and was due to the large errors in the angle and angular rate data. If these errors exceed the linearity region in the Kalman filter assumptions, a possible result is a biased estimate (Ref 7:348). To see if this was the case, an initial velocity with error magnitude of approximately 100 m/s was manually put into the program. The resulting mean radial

41

and velocity errors for the 50 cases are shown in Figures 11 and 12. The WLS mean errors were exactly the same as in the first 50 runs and are included so that the change of scale can be seen. These figures show that the mean errors for the smaller amounts of data do not experience the large errors observed in the original runs and that the negative bias observed has been reduced by nearly 50%. The most probable reason for the large errors and the bias is that the linearity assumptions were violated. The Kalman filter's sensitivity to non-linearities is discussed by Jazwinski (Ref 4:348). This example shows that WLS is apparently not as sensitive to non-linearity as the Kalman filter since it showed no biases or erratic results when used with the larger initial errors.

To determine non-linear effects in the WLS filter, several runs were made with progressively larger initial velocity errors. The WLS process showed no increased error until the initial velocity errors were in the 6000-7000 m/s range. Specifically, the filter diverged in all cases when the errors reached 6200 m/s and then no orbital elements were produced.

To see how errors of this magnitude affected the Kalman filter, cases were run with an initial velocity error of 7500 m/s. The resulting mean radial and velocity errors are shown in Figures 13 and 14. For 58 observations, the orbital periods produced ranged between 96.29636 and 96.30740 minutes. These values reflect an error range of 4.53 to 5.19 second. Thus, with initial error magnitudes larger than those which cause the Weighted Least Squares method to diverge and produce no usable results, the Kalman filter is still able to give relatively accurate estimates of the critical orbit element.

Computer Memory and Time Requirements

The CDC 660 central processor time required by each program to compute the final orbit was similar in most cases, with the Kalman filter being slightly faster.

For 10 data points, the time per case for the Kalman filter was 1.02 seconds and for WLS 1.29 seconds. For 58 data points, the time per case was 3.0 seconds for the Kalman filter and 5.19 seconds for the Least Squares filter.

The core storage requirements for one pass of data for the two programs were 67200 octal words for the Kalman filter and 60200 octal words for Least Squares. The majority of the space used by the Kalman filter was for the filter itself, whereas in the WLS filter a significant proportion of the memory was used for residual and matrix storage.
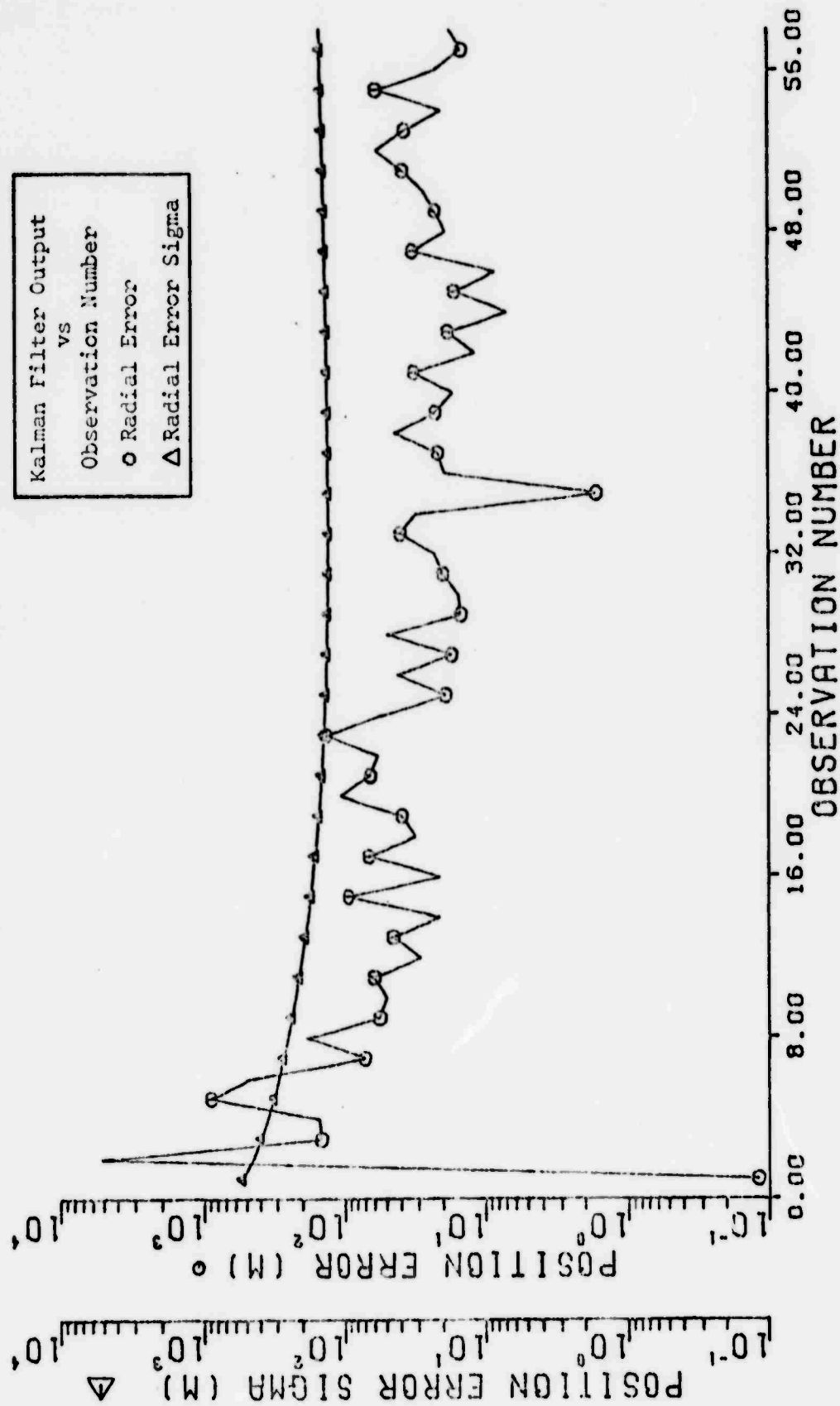
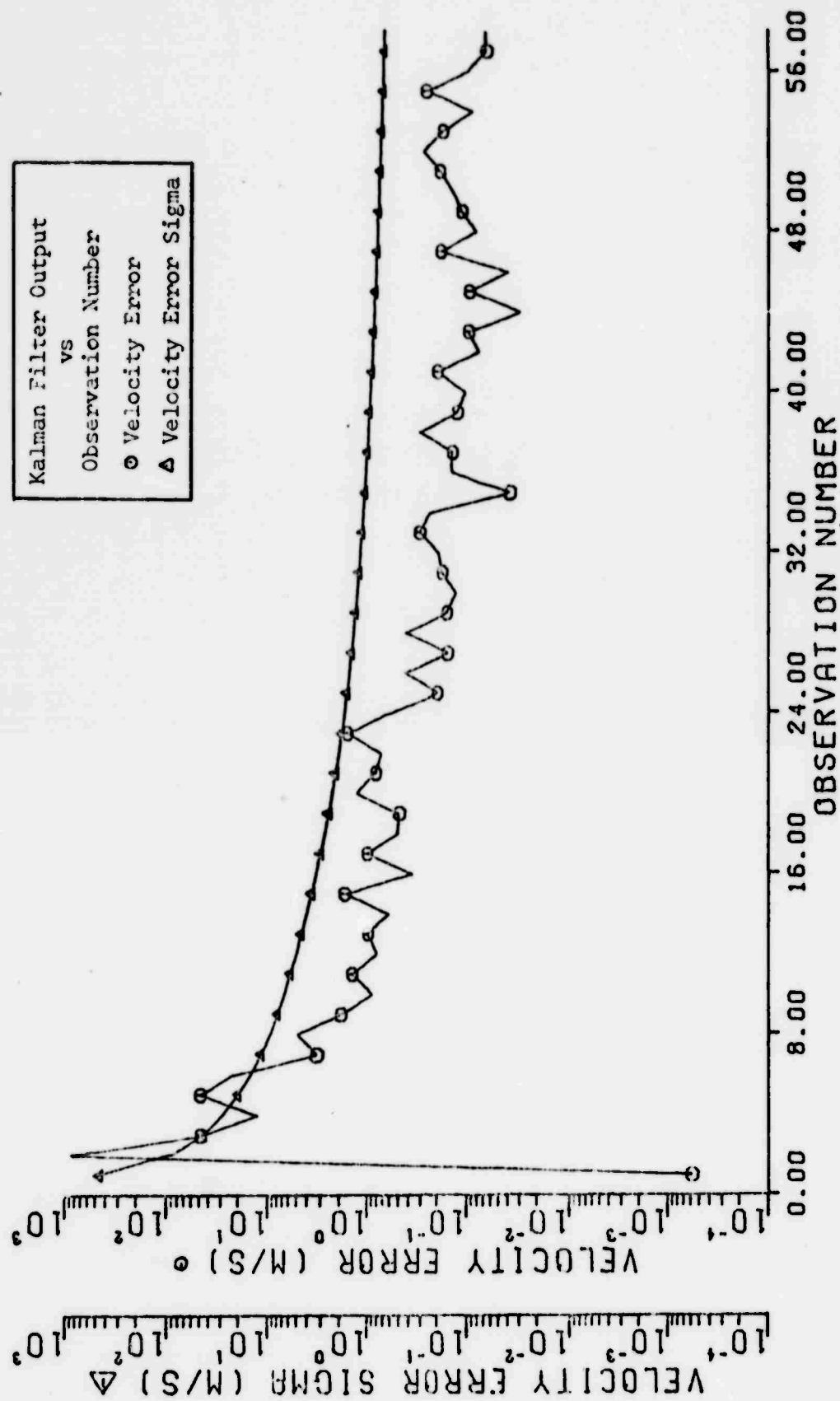Figure 5. Kalman Filter Estimated Radial Error and Sigma - Single Run

Figure 6. Kalman Filter Estimated Velocity Error and Sigma - Single Run
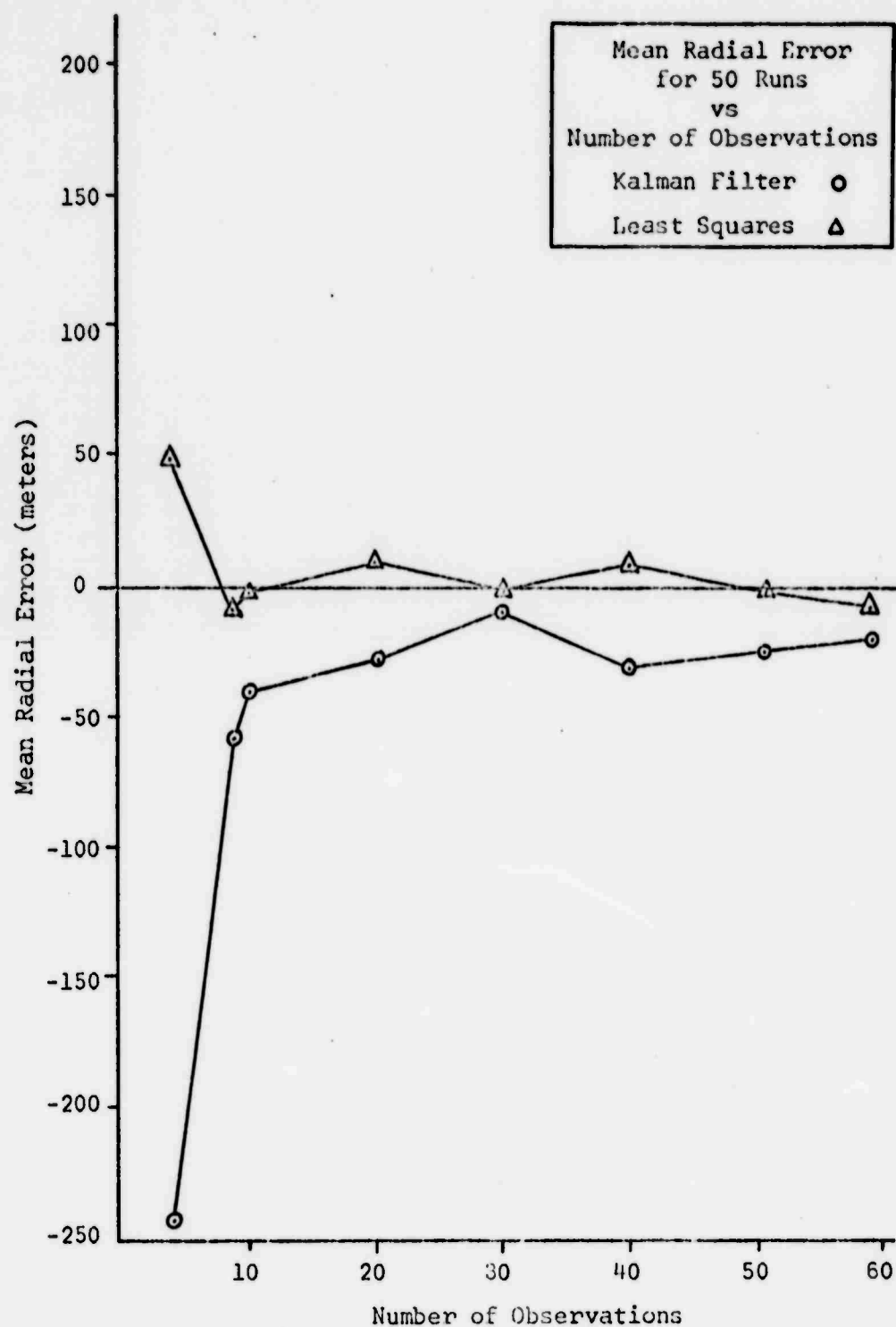
Figure 7. Kalman and Least Squares Mean Radial Error - 50 Runs
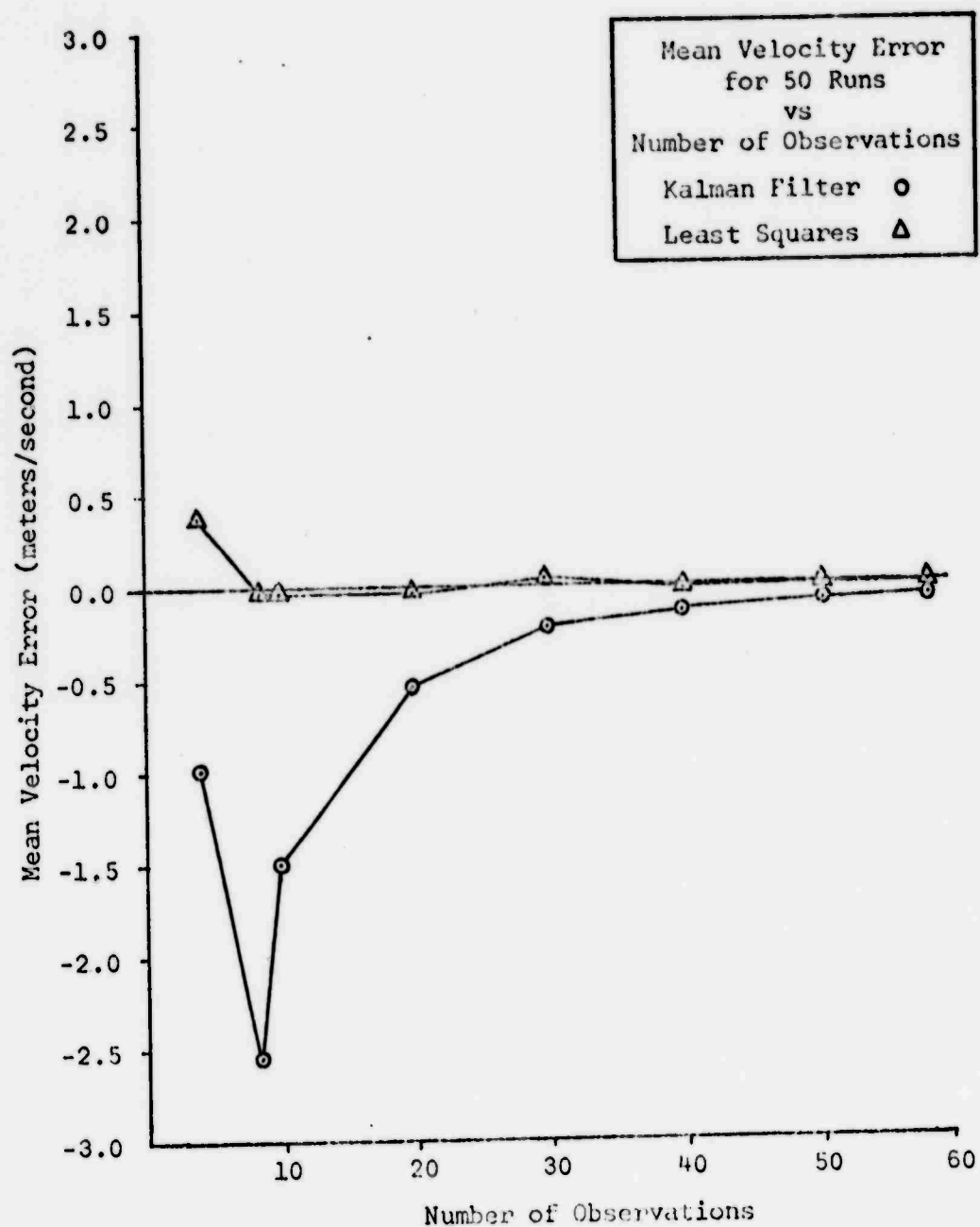
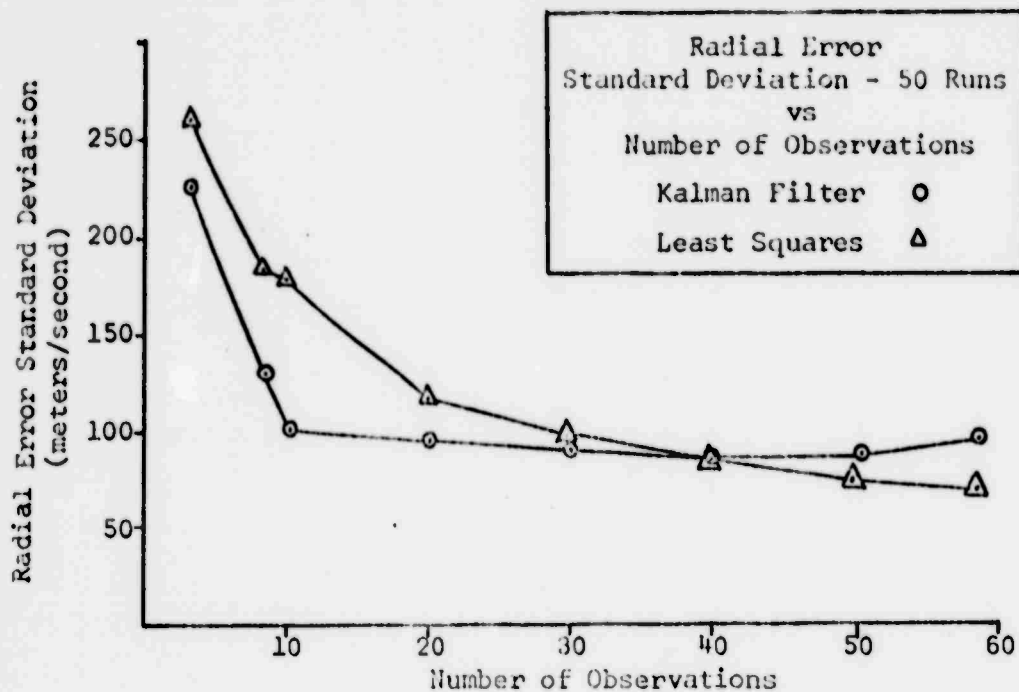Figure 8. Kalman and Least Squares Mean Velocity Error - 50 Runs

Figure 9. Kalman and Least Squares Radial Error
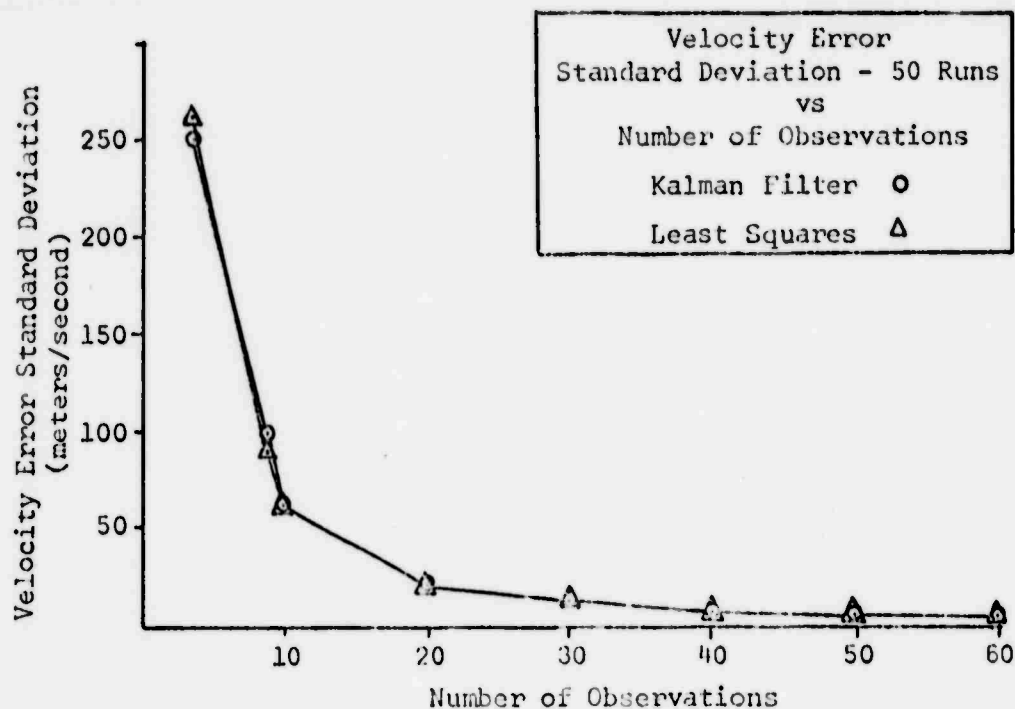Standard Deviation - 50 Runs

Figure 10. Kalman and Least Squares Velocity Error
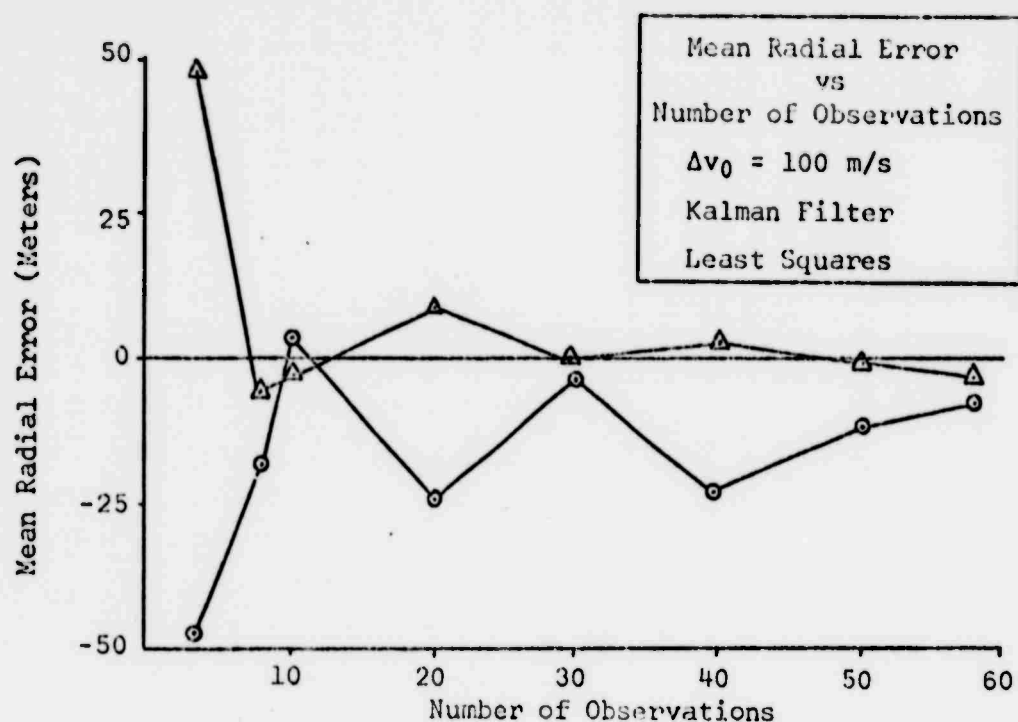Standard Deviation - 50 Runs

Figure 11. Kalman and Least Squares Mean Radial
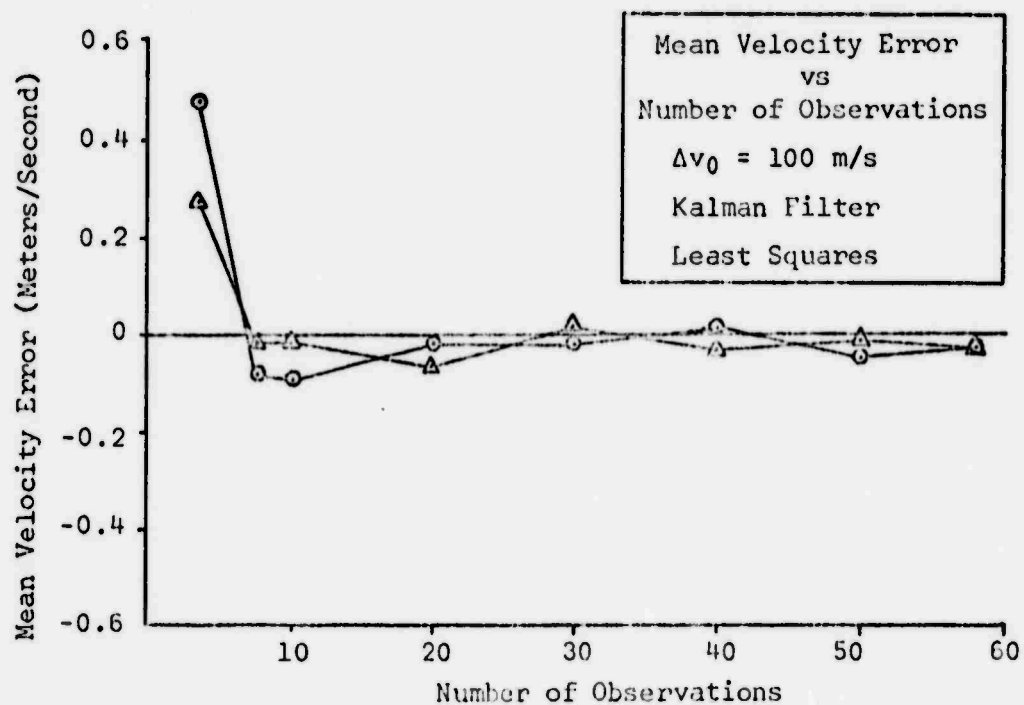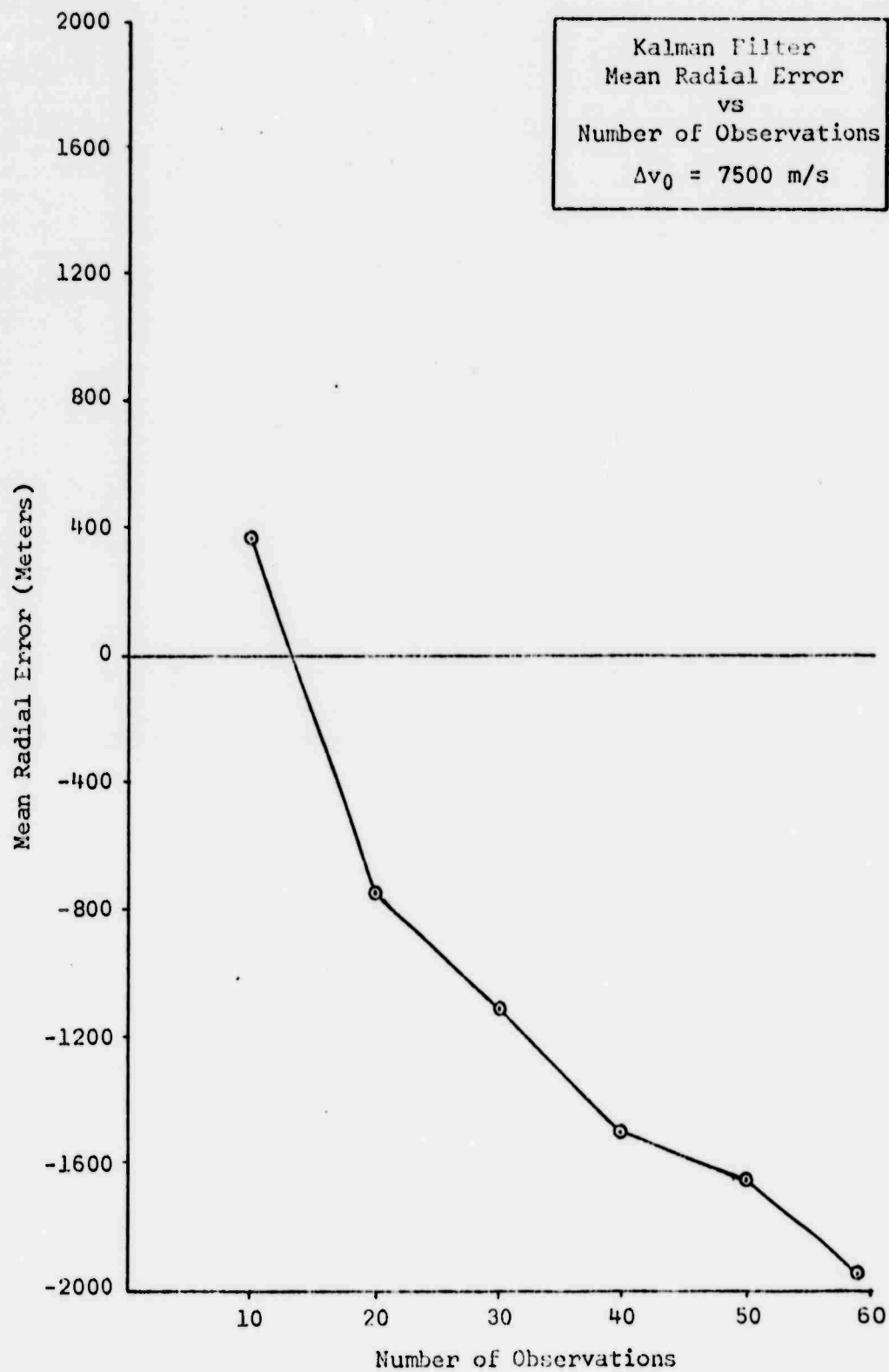Error, $\Delta v_0 = 100$ m/s

Figure 12. Kalman and Least Squares Mean Velocity
Error, $\Delta v_0 = 100$ m/s

Figure 13.   Kalman Filter Mean Radial Error, $\Delta v_0 = 7500$ m/s

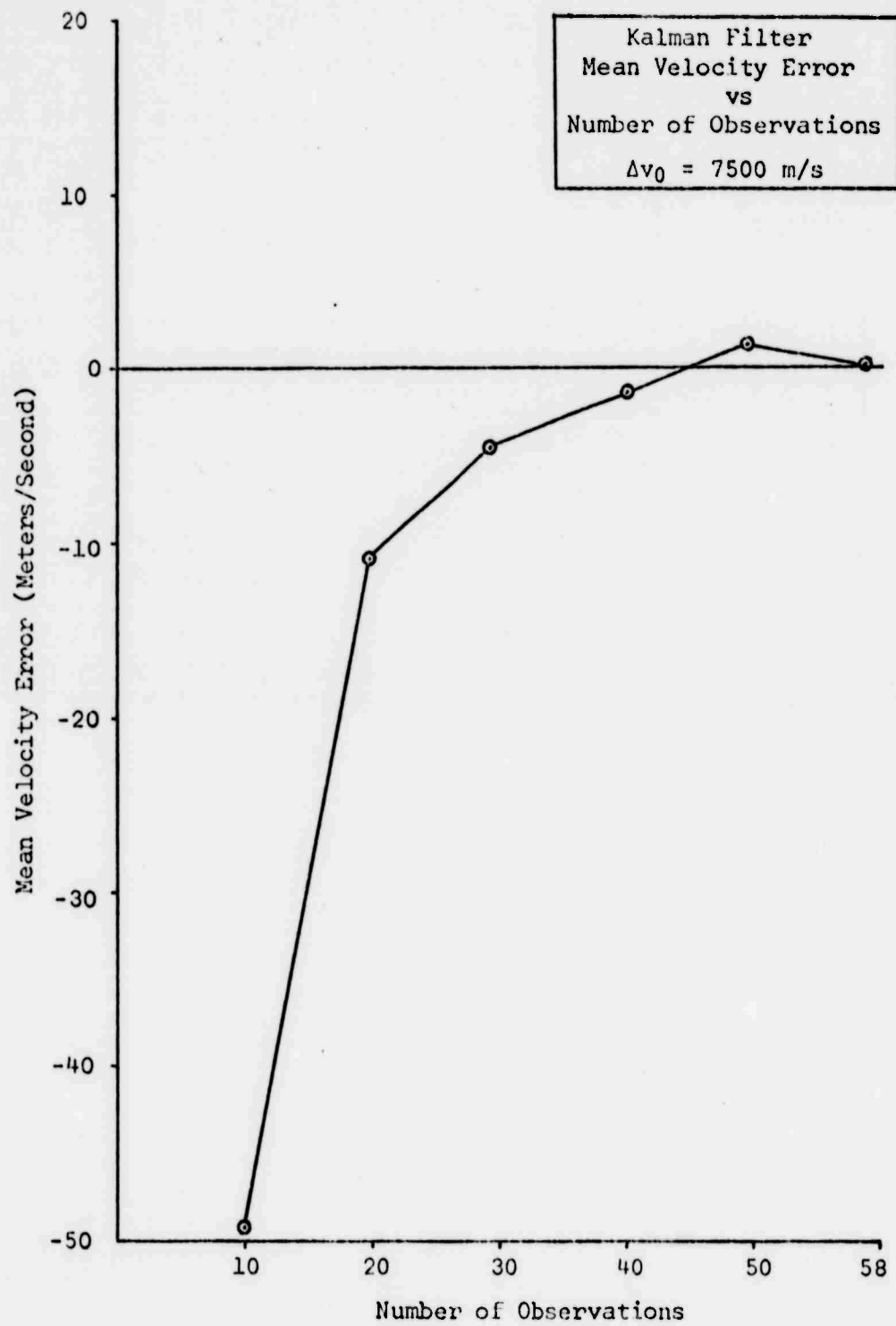Figure 14. Kalman Filter Mean Velocity Error, Δv_0 = 7500 m/s

VII. Conclusions and Recommendations

Conclusions

1. The Weighted Least Squares filter and the Extended Kalman filter produce extremely accurate results when applied to one-pass tracking data for a medium-altitude satellite where the model is known. The accuracy of both methods drops when fewer observations are used, but with as few as 10 observations usable answers are still produced.

2. For the orbit determination problem considered the Extended Kalman filter is more sensitive to non-linearities in the model than Weighted Least Squares and is more sensitive to initial condition errors. This sensitivity leads to relatively large mean errors in the early part of the process and an overall small bias as the process continues. These biases are not of a magnitude to seriously affect the resulting orbit parameters, but they do grow to fairly large magnitudes when the initial errors become very large. When these initial errors finally become large enough to cause divergence in the Weighted Least Squares process, the Kalman filter is still able to produce usable estimates.

3. The computer memory and central processor time requirements are similar for both methods.

Recommendations

The following topics are recommended for further study:

1. Apply the Extended Kalman filter and the Weighted Least Squares filter, using the same model, to data with different variances and to data from different orbits to continue the comparison.

2. Examine the present orbit model using Weighted Least Squares compared with the Extended Kalman filter with smoothing back to t_0.

3. Compare the two methods when applied to multiple passes of a satellite.

4. Examine the two filters when applied to the present model with known drag forces added

5. Apply the methods using the simple earth model to actual data and compare their handling of model errors.

6. Expand the two systems to employ the current known earth model and use them with actual data. These results could be compared with results from the previous recommended study.

7. Combine the two methods in a Limited Memory Filter as described in Reference 4 (pages 255-258). This method would combine the best points of each of the two methods.

Bibliography

1. Baker, Robert M.L. Astrodynamics. New York: Academic Press, Inc., 1967.

2. Escobal, Pedro R. Methods of Orbit Determination. New York: John Wiley and Sons, Inc., 1965.

3. Filiatreau, Thomas R. and George E. Elliott. Application of the Kalman Filter to Orbit Determination. Air Force Institute of Technology, Master Thesis, Wright-Patterson AFB, Ohio: June 1970.

4. Jazwinski, Andrew H. Stochastic Processes and Filtering Theory. New York: Academic Press, Inc., 1970.

5. Koskela, Paul E. Astrodynamic Analysis for the Advanced Orbit/ Ephemeris Subsystem. Aeronutronic Publication No. V-4180. Newport Beach, California: Philco-Ford Corporation, September 1967.

6. Meditch, J.S. Stochastic Optimal Linear Estimation and Control. New York: McGraw-Hill, 1969.

7. Prislin, R.H. Trace66 Orbit Determination Program, Volume V: Differential Correction Procedure and Techniques. Aerospace Report No. TOR-0066(9320)-2. VOL V. Los Angeles: The Aerospace Corporation, 1970.

8. Rogers, Charles E. and Christo Christodoulou. The Extended Kalman Filter Applied to the Determination of the Orbital Parameters of a Passive Earth Satellite. Air Force Institute of Technology, Master Thesis, Wright-Patterson AFB, Ohio: June 1971.

Appendix A

Determination of Initial Conditions

The equations used to produce the initial state estimate are presented in this appendix. The initial condition module needs the following data:

1. Tracking station height in earth radii: h

2. Tracking station latitude in degrees: ϕ

3. Tracking station longitude in degrees: θ

4. Slant range in meters: ρ

5. Slant range rate in meters/second: $\dot{\rho}$

6. Azimuth from north, clockwise, in degrees: a

7. Elevation in degrees: e

8. Azimuth rate in degrees/second: $\dot{a}$

9. Elevation rate in degrees/second: $\dot{e}$

Station Coordinates in Rotating Frame

$$\underline{R}_R = \begin{bmatrix} x_S \\ y_S \\ z_S \end{bmatrix}_R = \begin{bmatrix} (1+h)\cos(\theta)\cos(\phi) \\ (1+h)\sin(\theta)\cos(\phi) \\ (1+h)\sin(\phi) \end{bmatrix} \qquad (A-1)$$

$\underline{L}$ and $\underline{\dot{L}}$ in Rotating Frame

The vectors $\underline{L}$ and $\underline{\dot{L}}$ are unit vectors in the earth centered rotating frame representing the position and velocity of the satellite relative to the station.

$$\underline{L} = \begin{bmatrix} \ell_x \\ \ell_y \\ \ell_z \end{bmatrix}_R = \begin{bmatrix} (\ell_2 - \ell_1)\cos(\theta) - \ell_3\sin(\theta) \\ (\ell_2 - \ell_1)\sin(\theta) + \cos(\theta) \\ \cos(\phi)\cos(e)\cos(a) + \sin(\phi)\sin(e) \end{bmatrix} \quad (A-2)$$

where

$$\ell_1 = \sin(\phi)\cos(e)\cos(a) \quad\quad (A-3)$$

$$\ell_2 = \cos(\phi)\sin(e) \quad\quad (A-4)$$

$$\ell_3 = \cos(e)\sin(a) \quad\quad (A-5)$$

$$\underline{\dot{L}} = \begin{bmatrix} \dot{\ell}_x \\ \dot{\ell}_y \\ \dot{\ell}_z \end{bmatrix}_R \quad\quad (A-6)$$

where

$$\dot{\ell}_x = \dot{a}[\cos(\theta)\sin(\phi)\sin(a)\cos(e) - \cos(a)\sin(\theta)\cos(e)] +$$
$$\dot{e}[\cos(\theta)\sin(\phi)\sin(e)\cos(a) + \cos(\theta)\cos(\phi)\cos(e)] +$$
$$\dot{e}[\sin(\theta)\sin(a)\sin(e)] \quad\quad (A-7)$$

$$\dot{\ell}_y = \dot{a}[\sin(\theta)\sin(\phi)\sin(a)\cos(e) + \cos(a)\cos(\theta)\cos(e)] +$$
$$\dot{e}[\sin(\theta)\sin(\phi)\cos(a)\sin(e) + \sin(\theta)\cos(\phi)\cos(e)] -$$
$$\dot{e}[\cos(\theta)\sin(e)\sin(a)] \quad\quad (A-8)$$

$$\dot{\ell}_z = -\dot{a}[\cos(\phi)\sin(a)\sin(e)] +$$
$$\dot{e}[\sin(\phi)\cos(e) - \cos(\phi)\cos(a)\sin(e)] \quad\quad (A-9)$$

Satellite Position and Velocity in Rotating Frame

Once the unit vectors $\underline{L}$ and $\underline{\dot{L}}$ are determined, the satellite's position and velocity in the earth-centered rotating frame are

$$\underline{r}_R = \begin{bmatrix} x \\ y \\ z \end{bmatrix}_R = \rho \underline{L} + \underline{R}_R \tag{A-10}$$

and

$$\underline{\dot{r}}_R = \begin{bmatrix} \dot{x} \\ \dot{y} \\ \dot{z} \end{bmatrix}_R = \rho \underline{\dot{L}} + \dot{\rho} \underline{L} \tag{A-11}$$

These six components comprise the initial state vector $\underline{x}(0)$ in the rotating system. The initial state vector in the inertial system is then determined by

$$\underline{r}_I = \begin{bmatrix} x \\ y \\ z \end{bmatrix}_I = \begin{bmatrix} \cos(\omega t) & -\sin(\omega t) & 0 \\ \sin(\omega t) & \cos(\omega t) & 0 \\ 0 & 0 & 1 \end{bmatrix} \begin{bmatrix} x \\ y \\ z \end{bmatrix}_R \tag{A-12}$$

and

57

$$\underline{\dot{r}}_I = \begin{bmatrix} \dot{x} \\ \dot{y} \\ \dot{z} \end{bmatrix}_I = \begin{bmatrix} \cos(\omega t) & -\sin(\omega t) & 0 \\ \sin(\omega t) & \cos(\omega t) & 0 \\ 0 & 0 & 1 \end{bmatrix} \begin{bmatrix} \dot{x} \\ \dot{y} \\ \dot{z} \end{bmatrix}_R +$$

$$\begin{bmatrix} 0 & -\omega & 0 \\ \omega & 0 & 0 \\ 0 & 0 & 0 \end{bmatrix} \begin{bmatrix} x \\ y \\ z \end{bmatrix}_I \qquad\qquad (A-13)$$

Appendix B

State Sensitivity Matrix F

The state sensitivity matrix F, is used in the computation of the State Transition Matrix used in linearization schemes. F is defined as

$$F = \frac{f(x)}{\partial x} = \begin{bmatrix} \dfrac{\partial \dot{x}_1}{\partial x_1} & \dfrac{\partial \dot{x}_1}{\partial x_2} & \cdot & \cdot & \cdot & \dfrac{\partial \dot{x}_1}{\partial x_6} \\[2ex] \dfrac{\partial \dot{x}_2}{\partial x_1} & \dfrac{\partial \dot{x}_2}{\partial x_2} & \cdot & \cdot & \cdot & \dfrac{\partial \dot{x}_2}{\partial x_6} \\[2ex] \cdot & & & & & \cdot \\ \cdot & & & & & \cdot \\ \cdot & & & & & \cdot \\[2ex] \dfrac{\partial \dot{x}_6}{\partial x_1} & \dfrac{\partial \dot{x}_6}{\partial x_2} & \cdot & \cdot & \cdot & \dfrac{\partial \dot{x}_6}{\partial x_6} \end{bmatrix} \tag{B-1}$$

and, when the function $\underline{f}(\underline{x})$ is expressed in the inertial frame, the matrix F, neglecting zero terms is

$$F_{14} = F_{25} = F_{36} = 1 \tag{B-2}$$

$$F_{41} = \frac{\mu}{r^3} \left[3 \left(\frac{x}{r} \right)^2 - 1 \right] \tag{B-3}$$

$$F_{42} = \frac{\mu}{r^3} \left(\frac{3xy}{r^2} \right) \tag{B-4}$$

$$F_{43} = \frac{\mu}{r^3} \left(\frac{3xz}{r^2} \right) \tag{B-5}$$

$$F_{51} = \frac{\mu}{r^3}\left(\frac{3xy}{r^2}\right) \tag{B-6}$$

$$F_{52} = \frac{\mu}{r^3}\left[3\left(\frac{y}{r}\right)^2 - 1\right] \tag{B-7}$$

$$F_{53} = \frac{\mu}{r^3}\left(\frac{3yz}{r^2}\right) \tag{B-8}$$

$$F_{61} = \frac{\mu}{r^3}\left(\frac{3xz}{r^2}\right) \tag{B-9}$$

$$F_{62} = \frac{\mu}{r^3}\left(\frac{3yz}{r^2}\right) \tag{B-10}$$

$$F_{63} = \frac{\mu}{r^3}\left[3\left(\frac{z}{r}\right)^2 - 1\right] \tag{B-11}$$

When the function $\underline{f}(\underline{x})$ is expressed in rotating coordinates, the F matrix, again neglecting zero terms, is

$$F_{14} = F_{25} = F_{36} = 1 \tag{B-12}$$

$$F_{41} = \frac{\mu}{r^3}\left[3\left(\frac{x}{r}\right)^2 - 1\right] + \omega^2 \tag{B-13}$$

$$F_{42} = \frac{\mu}{r^3}\left(\frac{3xy}{r^2}\right) \tag{B-14}$$

$$F_{43} = \frac{\mu}{r^3}\left(\frac{3xz}{r^2}\right) \tag{B-15}$$

$$F_{45} = 2\omega \tag{B-16}$$

$$F_{51} = \frac{\mu}{r^3} \left(\frac{3xy}{r^2} \right) \tag{B-17}$$

$$F_{52} = \frac{\mu}{r^3} \left[3 \left(\frac{y}{r} \right)^2 - 1 \right] + \omega^2 \tag{B-18}$$

$$F_{53} = \frac{\mu}{r^3} \left(\frac{3yz}{r^2} \right) \tag{B-19}$$

$$F_{54} = -2\omega \tag{B-20}$$

$$F_{61} = \frac{\mu}{r^3} \left(\frac{3xz}{r^2} \right) \tag{B-21}$$

$$F_{62} = \frac{\mu}{r^3} \left(\frac{3yz}{r^2} \right) \tag{B-22}$$

$$F_{63} = \frac{\mu}{r^3} \left[3 \left(\frac{z}{r} \right)^2 - 1 \right] \tag{B-23}$$

Appendix C

Measurement Matrix M

The measurement matrix M, consists of the partial derivatives of the measurements ρ, $\dot{\rho}$, a, and e with respect to the state vector $\underline{x}$. If the state vector is in rotating coordinates, M is

$$M_R = \left[\frac{\partial h(\underline{x})}{\partial \underline{x}} \right]_R = \begin{bmatrix} M(1) \\ M(2) \\ M(3) \\ M(4) \end{bmatrix}_R \qquad (C-1)$$

where M(1), M(2), M(3), and M(4) are row vectors and are

$$M(1) = \frac{1}{\rho} [x_R - x_S, \; y_R - y_S, \; z_R - z_S, \; 0, \; 0, \; 0] \qquad (C-2)$$

$$M(2) = \frac{1}{\rho} \left[\dot{x}_R - \frac{\dot{\rho}(x_R - x_S)}{\rho}, \; \dot{y}_R - \frac{\dot{\rho}(y_R - y_S)}{\rho}, \; \dot{z}_R - \right.$$

$$\left. \frac{\dot{\rho}(z_R - z_S)}{\rho}, \; x_R - x_S, \; y_R - y_S, \; z_R - z_S \right] \qquad (C-3)$$

$$M(3) = \left[\frac{1}{(x_T^2 + y_T^2)} \right] [-x_T \sin(0) - y_T \sin(\;)\cos(\theta), \; x_T \cos(0) -$$

$$y_T \sin(\theta)\sin(\phi), \; y_T \cos(\phi), \; 0, \; 0, \; 0] \qquad (C-4)$$

$$M(4) = \left[\frac{1}{(x_T^2 + y_T^2)^{1/2}} \right] \left[\cos(\phi)\cos(\theta) - \frac{z_T(x_R - x_S)}{\rho^2} , \sin(\theta)\cos(\phi) - \right.$$

$$\left. \frac{z_T(y_R - y_S)}{\rho^2} , \sin(\phi) - \frac{z_T(z_R - z_S)}{\rho^2} , 0, 0, 0 \right] \qquad (C-5)$$

If the state vector is in inertial coordinates, the matrix M is

$$M_I = M_R \begin{bmatrix} \cos(\omega t) & \sin(\omega t) & 0 & 0 & 0 & 0 \\ -\sin(\omega t) & \cos(\omega t) & 0 & 0 & 0 & 0 \\ 0 & 0 & 1 & 0 & 0 & 0 \\ -\omega\sin(\omega t) & \cos(\omega t) & 0 & \cos(\omega t) & \sin(\omega t) & 0 \\ \omega\cos(\omega t) & -\sin(\omega t) & 0 & -\sin(\omega t) & \cos(\omega t) & 0 \end{bmatrix} \qquad (C-6)$$

Vita

Jackson R. Ferguson Jr. was ███████████ ████ █████ ███████████ He graduated from ███████ ███████████████ Austin, Texas in 1960 and entered the University of Texas where he majored in Electrical Engineering until June 1961, when he entered the United States Air Force Academy at Colorado Springs, Colorado. He graduated with a Bachelor of Science degree in Engineering Science in June 1965. After a six month tour at Webb Air Force Base, Texas, he was assigned to Detachment 1, Air Force Satellite Control Facility, Sunnyvale, California as a Satellite Test Planning Officer from January 1966 until his entry into the Air Force Institute of Technology in June 1970.

Permanent address: ███████████████ ███████████

This thesis was typed ██████ █████████████